JCZ: Zoologischer Anzeiger - A Journal of Comparative Zoology 307 (2023) 36–53

Contents lists available at ScienceDirect

Zoologischer Anzeiger

journal homepage: www.elsevier.com/locate/jcz

Messor erwini sp. n., a hitherto cryptic harvester ant in the Iberian Peninsula

Noel Orou [a,1], Sándor Csősz [b,c,1], Xavier Arnan [d,e], Rodrigo G. Pol [f,g], Wolfgang Arthofer [a,h], Birgit C. Schlick-Steiner [a,*,2], Florian M. Steiner [a,2]

[a] Universität Innsbruck, Department of Ecology, Technikerstraße 25, 6020, Innsbruck, Austria
[b] MTA-ELTE-MTM Ecology Research Group, Pázmány Péter sétány 1/C, 1117, Budapest, Hungary
[c] Evolutionary Ecology Research Group, Institute of Ecology and Botany, Centre for Ecological Research, Vácrátót, Hungary
[d] CREAF Centre for Ecological Research and Forestry Applications, Autonomous University of Barcelona, 08193, Cerdanyola del Vallès, Spain
[e] Universidade de Pernambuco – Campus Garanhuns, R. Padre Agobar Valença, s/n - Severiano Moraes Filho, Garanhuns, PE, 55299-390, Brazil
[f] Desert Community Ecology Research Team (Ecodes), IADIZA-CONICET, 5500, Mendoza, Argentina
[g] Facultad de Ciencias Exactas y Naturales, Universidad Nacional de Cuyo, 5500, Mendoza, Argentina
[h] Praxis für Humangenetik, Brünnlbadgasse 15, 1090, Vienna, Austria

ARTICLE INFO

Keywords:
Cryptic species
Species delimitation
Microsatellites
mtDNA
Morphometrics

ABSTRACT

European harvester ants, *Messor* species, are important ecosystem engineers. In Catalonia (Spain), among others, the three species *Messor barbarus*, *M. bouvieri*, and *M. capitatus* occur. At one Catalan site, a cluster of nest samples of unknown identity was found, raising the possibility of either a hybrid lineage or a currently unexplored species in the region. The aim of this study was to test whether the newly recognized cluster represents a hybrid of *M. barbarus* and *M. capitatus*, or some form of social hybridogenesis, or an independent, hitherto unrecognised species. We addressed this question in an integrative taxonomic fashion combining evidence from microsatellites analyzed via Bayesian cluster analysis, phylogenetic analyses based on mitochondrial DNA, and multivariate exploratory and confirmatory analyses of morphometric data. The unidentified *Messor* ants formed a well separated entity from *M. barbarus*, *M. capitatus*, and *M. bouvieri* in all these analyses. These results are in line with the existence of a cryptic *Messor* species but not with hybridization nor social hybridogenesis. The newly detected species, which has been neither genetically nor morphologically analyzed before, is described as *Messor erwini* sp. n., since no name-bearing types of valid *Messor* taxa correspond with the morphological characteristics of the species. Discovering a hitherto unknown species from a myrmecologically well studied area nourishes expectations that further diversity of the genus *Messor* may await its discovery.

1. Introduction

Harvester ants including those of the genus *Messor* Forel, 1890 play an important role in grassland ecosystems. As major seed consumers in xeric grasslands and shrublands, they collect huge numbers of plant seeds and store them in underground granaries (Hölldobler and Wilson 1990; Westerman et al., 2012) Thus, they influence the vegetation by dispersing seeds and reducing seed banks (Arnan et al., 2010). Furthermore, they affect the physical, chemical, and hydrological properties of the soil (Cammeraat et al., 2002) by facilitating the organic carbon and nutrient cycle (Plowes et al., 2013). The genus *Messor* is distributed in the holarctic, the palaeotropical, and the oriental region and includes about 127 species (Bolton 2022). For the Iberian peninsula, 11 species have been listed (Borowiec 2014). In the genus *Messor*, various evolutionary phenomena have been studied, including cryptic speciation (Steiner et al., 2018), hybridization (Steiner et al., 2011), and social hybridogenesis (Norman et al., 2016; Romiguier et al., 2017).

Morphologically cryptic species complicate species delimitation – they are morphologically similar and hardly to distinguish as interspecific differences are small and intraspecific variation is high (Wiens 1999; Puechmaille 2016). Therefore, genetic analyses are a helpful tool to postulate hypotheses for species classification (Bickford et al., 2007), which can be tested using integrative-taxonomy approaches (Schlick-Steiner et al., 2010; Dejaco et al., 2016). In ants generally (Lucas et al.,

* Corresponding author.
E-mail address: birgit.schlick-steiner@uibk.ac.at (B.C. Schlick-Steiner).
[1] These authors contributed equally to this work as first authors.
[2] These authors contributed equally to this work as senior authors.

https://doi.org/10.1016/j.jcz.2023.09.001
Received 16 February 2022; Received in revised form 10 August 2023; Accepted 1 September 2023
Available online 9 September 2023

2002; Knaden et al., 2005; Ross et al., 2010; Csősz et al., 2014; Seifert et al., 2014) and also in the genus *Messor* (Schlick-Steiner et al., 2006; Steiner et al., 2018), several cryptic species were revealed in the past. Steiner et al. (2018) identified five cryptic species in the European *Messor structor* (Latreille, 1798) by conducting a multidisciplinary approach, which included an analysis of cytochrome c oxidase subunit I (COI) (mitochondrial DNA, mtDNA), amplified fragment length polymorphisms (nuclear DNA), and a morphometric analysis (Steiner et al., 2018).

Interspecific hybridization is common in nature; reportedly 10–30% of multicellular animal and plant species are known to form hybrids on the per-species basis (Abbott et al., 2013). In ants, it is widely spread and often produces fertile hybrids which then backcross (Seifert, 1999; Mallet, 2005; Seifert, 2019a; 2019b). Hybridization has also already been described for *Messor*: Steiner et al. (2011) explored this in central and south Italian populations of the three sympatric species *Messor minor* (André, 1883), *Messor* cf. *wasmanni* Krausse, 1910, and *Messor capitatus* Latreille, 1798 (Baroni Urbani 1971; Solida et al., 2010). With molecular methods, using microsatellites (nuclear DNA) and COI, combined with a morphometric analysis, they revealed a bidirectional interspecific gene flow through hybridization between the co-occurring *M. minor* and *M.* cf. *wasmanni* (Steiner et al., 2011). In other instances, hybrid populations were found to be ecologically separated from the parental species, potentially resulting in hybrid speciation (butterfly example: Gompert et al., 2006).

There also exists intraspecific hybridization between two different lineages of one *Messor* species as part of a reproduction mode called social hybridogenesis, as studied by Romiguier et al. (2017) in southwestern Europe. While queens produce queens by mating with males of their own lineage, they produce workers by mating with males of the other lineage. Workers then can also produce males through parthenogenesis. Social hybridogenesis is possibly linked to the peculiar ecology of harvester ants. As strict granivores (Fiedler et al., 2007), they are not able to control caste determination by feeding the larvae with different diet, so they use this reproduction mode mating with different genetic lineages instead (Romiguier et al., 2017). Social hybridogenesis has so far been detected in *Messor barbarus* (Linnaeus, 1767) (Norman et al., 2016), *Messor ebeninus* Santschi, 1927, and *M. structor*, but not in *M. capitatus* and other species (Romiguier et al., 2017).

In Catalonia, in the northeast of Spain, *M. barbarus*, *Messor bouvieri* Bondroit, 1918, and *M. capitatus* are by far the most widely distributed and active *Messor* species (Bernhard 1968; Arnan et al., 2006; Arnan et al., 2010; Lebas et al., 2016). In myrmecological routine prior to this study, their identification has been based on some salient morphological features (but see section "5.2. Formal descriptions of Iberian *Messor* species (alphabetic order)" for the state of knowledge resulting from this study): psammophore (J-shaped hairs on the underside of the head forming a structure resembling a "beard") present in *M. bouvieri* but absent in the other two species; major workers of *M. barbarus* with red head and rounded propodeum; major workers of *M. capitatus* concolorous black and with angled propodeum (Collingwood 1976; Cagniant and Espadaler 1998; Collingwood 1998). The three species also differ in the degree of worker-size polymorphism in that *M. barbarus* and *M. capitatus* colonies are much more polymorphic than *M. bouvieri*, which lacks the largest worker size (Arnan et al., 2010). Finally, the three species also differ clearly in their foraging behavior: *M. capitatus* workers predominantly forage individually, in contrast to the other two species, which form trails, *M. barbarus* permanent and *M. bouvieri* temporary ones (Cerdá and Retana 1994; Arnan et al., 2010; Plowes et al., 2013).

At a Catalonian site, three *Messor* species co-occur with high colony densities, and their species identities have been documented in the literature as *M. barbarus*, *M. bouvieri*, and *M. capitatus* (Arnan et al., 2006; Arnan et al., 2010). Increasingly, however, doubts arose about the true species identity of colonies identified as "*M. capitatus*" as they were found to not strictly correspond to that species according to the current literature on species identification (Gómez and Espadaler 2007). Some major workers of this unidentified cluster of nest samples showed a scrambled trait combination: some diagnostic traits, such as a red head, were reminiscent of *M. barbarus*, while others, such as an angulate propodeum, were typical of *M. capitatus*. The size of bigger major workers was bigger than that of the largest species, *M. capitatus*, but foraging behavior was *M. barbarus*-like, as they were observed to form foraging trails. Altogether, this implied the chance of seeing a hybrid population. However, the unidentified *Messor* ants could alternatively represent a separate, cryptic species or the phenomenon of hybridogenesis.

Here, we set out to test the hypotheses of the three described evolutionary phenomena known in *Messor*. This was done by using an integrative approach containing microsatellites, COI, and morphometrics and including all three co-occurring *Messor* ants, given that complex scenarios are known for co-occurring *Messor* species from other regions (Steiner et al., 2011). Our study hypotheses were as follows: (i) "the new lineage is a separate species" hypothesis – in the data from all methods, the unidentified *Messor* population would form a well separated entity (cf. Steiner et al., 2018); (ii) "the new lineage is a hybrid" hypothesis that assumes hybridization between the two species of which the unidentified *Messor* ants combine morphological character states, that is, *M. barbarus* and *M. capitatus*, albeit based on morphology, it could not be excluded that also *M. bouvieri* would be involved – the microsatellites of the unidentified *Messor* would show an admixture of these two species, while in COI, the unidentified *Messor* would be assigned to the one species representing the maternal side; in morphometrics, it would be identified as intermediate between the two species (cf. Steiner et al., 2011); (iii) "social hybridogenesis" hypothesis, as already known for *M. barbarus* – in microsatellites, workers of the unidentified *Messor* would all have the same genotypes, while they would fall into two phylogenetic clusters in COI that would represent the two lineages involved (cf. Romiguier et al., 2017). To assess the situation at the site in Catalonia, we sampled all three *Messor* ants co-occurring on that spot. Evaluating the three hypotheses resulted in clear support of hypothesis (i), that is, the unidentified *Messor* population represents a separate, hitherto unrecognized species. We hereby describe this species as *Messor erwini*. sp. n. Currently, we know only little on the ecology and distribution of the species, but our work builds the basis for a better characterisation of these aspects in the future.

2. Material and methods

2.1. Sampling

The focal study area was an open and heterogeneous shrubland located in Castellbell i el Vilar, Barcelona (central Catalonia, northeast Spain, 41° 39′ N, 1° 51' E, Fig. 1), at 260 m above sea level, where the climate is typically Mediterranean, with a mean annual temperature of 14.5 °C and a mean annual precipitation of 565 mm. The vegetation type was the consequence of recurring fires in a *Pinus halepensis* (Mill.) forest. The pine forest did not recover after the last fire in 2003, and the area remained open. The fieldwork was conducted between 2018 and 2019, and vegetation consisted of alternating bare soil areas, grassland areas dominated by *Brachypodium phoenicoides* (L.) Roem. & Schult., *Brachypodium retusum* (Pers.) P.Beauv., and *Aphyllantes monspelienses* L., and areas with small (*Thymus vulgaris* L., *Coronilla minima* L.) and large-sized shrubs (*Pistacea lentiscus* L., *Rosmarinus officinalis* L., *Dorycnium pentaphyllum* Scop.). The study plot of about 6000 m^2 was located on a 10° southwest facing slope. In 2018, the numbers of nests known in the study plot of *M. barbarus*, *M. bouvieri*, and the unidentified *Messor* were 13, 27, and 55, respectively (X. Arnan, unpublished). From these nests, 10 to 20 workers each of eight colonies each of the species *M. barbarus* and *M. bouvieri* as well as three to 20 workers each of 18 nests of the unidentified *Messor* were sampled from June to July 2018 (Table S1).

At additional sites spread all over Catalonia, about 20 workers each

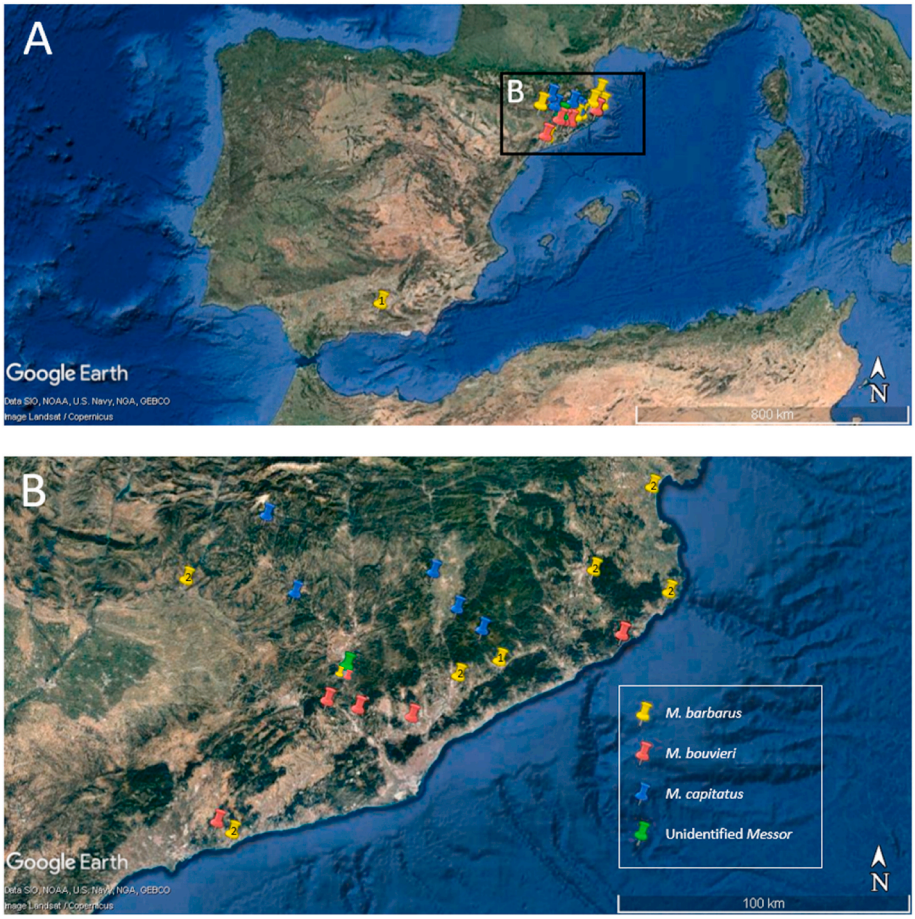

Fig. 1. Sampling sites. (A) Iberian peninsula; (B) Catalonia. Occurrences of *Messor barbarus* (yellow, subclades 1 and 2 as defined by Romiguier et al., 2017), *M. bouvieri* (red), *M. capitatus* (blue), and the hitherto unidentified *M. erwini* sp. n. (green) depicted; at the focal study area Castellbell i el Vilar, *M. barbarus*, *M. bouvieri*, and the unidentified *Messor* co-occur (Google Earth Pro 2019, Data SIO, NOAA, U.S. Navy, NGA, GEBCO, Image Landsat/Copernicus).

of eight nests of putative pure-species status (based on morphological character traits, Gómez and Espadaler 2007) of each of the three species *M. barbarus*, *M. bouvieri*, and *M. capitatus* were sampled from July to September 2018; the same applied to one additional *M. barbarus* nest in Andalusia (Fig. 1, Supplementary Data 1). These sampling sites were separated from each other by a minimum distance of 15 km. At each of these sites, only nests of one of the three species were detectable and collected, and collecting potential hybrids was thereby avoided.

All samples were stored in $EtOH_{abs}$. The species were identified using the key of Gómez and Espadaler (2007). From the focal study area, 18 colonies of the unidentified *Messor* were used for the analyses. Of these, one to eight workers per colony (for details, see Table S1) were used in the analyses. Further from the focal study area, each eight colonies were randomly chosen from the colonies sampled of *M. barbarus* and *M. bouvieri*, and of these 16 colonies, each one worker was used in the analyses. From the additional sites, eight colonies each of the three species *M. barbarus*, *M. bouvieri*, and *M. capitatus* were chosen, and of these 24 colonies, eight workers per colony were used (Table S1). Workers were chosen to represent the whole range of variation in body size and color as seen in a particular colony.

2.2. DNA extraction

For DNA extraction, only the gasters were used to save up the rest of the specimens for the morphometric analysis. DNA was extracted using the Qiagen DNeasy blood and tissue kit (Qiagen, Hilden, Germany) following the instructions of the manufacturer, except that the elution volume was increased to 100 µl.

2.3. Microsatellites

Specific primers for nine microsatellite loci, Mmap011, Mmap057, Mmap060, Mmap071, Mmap086, Mmap091, Mmap120, Mmap144, and Mmap148 (Table 1), were developed. In more detail, of *M. barbarus*, *M. bouvieri*, and *M. capitatus*, DNA of each one individual was extracted as described in Section 2.2. Extracted DNA was sent to a commercial provider for PE250 sequencing on an Illumina MiSeq next generation sequencer. Reads containing microsatellites were identified using the software SciRoKo (Kofler et al., 2007) and custom Phython scripts. Primers were designed using Primer3 (http://bioinfo.ut.ee/primer3-0.4.0/). All forward primers contained a 5′ M13 tail for subsequent fluorescent labeling. Additionally, six primer pairs originally developed for *M. structor* (Arthofer et al., 2005) were used, Ms24B, Ms13J, Ms1A, Ms2A, Ms2C, and Ms2D (Table 2).

PCRs were performed in 5 µl total reaction volume containing 1× RotorGene Probe PCR Kit, 0.02 µM forward primer, 0.2 µM reverse and M13 primers, and 0.5 or 1 µl template DNA. The M13 primers were 5′ labeled with either FAM, HEX, NED, or PET. PCR conditions were an initial denaturation step at 94 °C for 5 min, 32 or 40 cycles with 94 °C for 30 s, 50, 51, or 55 °C for 1 min, and 72 °C for 45 s, and a final extension step at 68 °C for 20 min. The used template DNA volumes, annealing temperatures, cycle numbers, and labels depended on the corresponding loci (Table 3). PCR success was controlled by agarose gel electrophoresis. Three or four PCR products with different fluorescent labels were mixed for fragment analysis (Table 3), which was conducted by the DNA Sequencing & Genotyping Facility, University of Chicago, USA.

Microsatellite genotyping was successful in 286 workers (one to

Table 1
Newly developed microsatellite primers for *Messor*. Primer ID, sequence, primer length in base pairs (bp), motif, amplicon length (bp), and GenBank accession number.

Primer ID	Sequence	Primer length (bp)	Motif	Amplicon length (bp)	GenBank accession number
Mmap011f	5′ CACGACGTTGTAAA ACGACCAACAGGTGTAAACTCGCG 3′	38	(CTT)7	231	MT492492
Mmap011r	5′ AAGTCGCTCATGAT TCTGC 3′	19			
Mmap057f	5′ CACGACGTTGTAAA ACGACCAACCGCGCTAAACTGAACT 3′	39	(AG)9	153	MT492493
Mmap057r	5′ CCGTCCCTGAGCAA TCAATA 3′	20			
Mmap060f	5′ CACGACGTTGTAAA ACGACCACGTGGTATTGATCGCAGG 3′	39	(CG)12	217	MT492494
Mmap060r	5′ CGGGGATAAGGGA GATCTGG 3′	20			
Mmap071f	5′ CACGACGTTGTAAA ACGACGAGTACGGAAGATAGGCAGGG 3′	40	(AC)9	207	MT492495
Mmap071r	5′ ATCGGTCAAGTGCG TGAGTA 3′	20			
Mmap086f	5′ CACGACGTTGTAAA ACGACAGGTCCGCATACTATCGAC 3′	38	(CGG)13	235	MT492496
Mmap086r	5′ ATAAGCACATCATC GACCGC 3′	20			
Mmap091f	5′ CACGACGTTGTAAA ACGACCGTCGCACTGCCATAATTGAG 3′	40	(CT)8	178	MT492497
Mmap091r	5′ GTAGAAAGAAAGA CAGGGTGCG 3′	22			
Mmap120f	5′ CACGACGTTGTAAA ACGACCCGACAAAGCGCTTACAGAAC 3′	40	(CT)21	243	MT492498
Mmap120r	5′ AAGGGCAGAAAAC GAACGAC 3′	20			
Mmap144f	5′ CACGACGTTGTAAA ACGACCGGTTTTCGTCTGCGTGAC 3′	38	(AG)10	252	MT492499
Mmap144r	5′ TGTTCGGTGACTGG AGTTCAG 3′	21			
Mmap148f	5′ CACGACGTTGTAAA ACGACCCCGCGTCCTGATTGAAAAT 3′	39	(AC)12	178	MT492500
Mmap148r	5′ ACATCGGAGGGTGT GTCTG 3′	19			

Table 2
Microsatellite primers originally developed for *Messor structor*. Primer ID, sequence, primer length in base pairs (bp), and reference.

Primer ID	Sequence	Primer length (bp)	Reference
Ms24Bf	5′ CCTTTGCCGTGAAAATC 3′	17	unpublished, EU441277
Ms24Br	5′ ATCGATTATCGCCTGAGC 3′	18	
Ms13Jf	5′ GGATCGTTCCCTCTTCGTT 3′	19	unpublished, EU441278
Ms13Jr	5′ CAGGGATTTGCGTGACCTAT 3′	20	
Ms1Af	5′ TGATACGAGCGAGTGGAAC 3′	19	Arthofer, W., Schlick-Steiner, B.C., Steiner, F.M., Konrad, H., Espadaler, X., Stauffer, C. (2005)
Ms1Ar	5′ TCCGTTTTTGTAGTGCGTC 3′	19	
Ms2Af	5′ CACGTAGGACGAACGTTG 3′	18	Arthofer, W., Schlick-Steiner, B.C., Steiner, F.M., Konrad, H., Espadaler, X., Stauffer, C. (2005)
Ms2Ar	5′ TAGAAATGGGTAGGCGTTCG 3′	20	
Ms2Cf	5′ CGTGCTTTGAGGAAGGGAT 3′	19	Arthofer, W., Schlick-Steiner, B.C., Steiner, F.M., Konrad, H., Espadaler, X., Stauffer, C. (2005)
Ms2Cr	5′ AGCCTCTCTGTCTTGTTCTC 3′	20	
Ms2Df	5′ CGGCACGGAGACAATACTTC 3′	20	Arthofer, W., Schlick-Steiner, B.C., Steiner, F.M., Konrad, H., Espadaler, X., Stauffer, C. (2005)
Ms2Dr	5′ GCTGTTCGGCGAAAACTATC 3′	20	

eight per colony; on average, 4.9 ± 3.4 standard deviation). Allele calling was performed manually using PeakScanner v.1.0 (Applied Biosystems). Genepop on the Web (Raymond and Rousset 1995; Rousset 2008) was used to calculate the allele frequencies and to test the Linkage Disequilibrium and Hardy–Weinberg Equilibrium. The p-values were Bonferroni-Holm corrected adapting an alpha of 0.05.

A Bayesian cluster analysis was conducted with STRUCTURE v.2.3.4 (Pritchard et al., 2000) using 20,000 burnin steps and 180,000 MCMC iterations after burnin. Each K from 1 to 6 was calculated 10 times. The primary STRUCTURE output was further processed using STRUCTURE Harvester (Earl and von Holdt 2012) implementing the method of Evanno et al. (2005). The STRUCTURE analysis was repeated after the exclusion of five loci that were in Linkage Disequilibrium (see 3.1. Microsatellites). Another STRUCTURE analysis was done using all loci except one with a high portion of missing data (Mmap144) and additionally excluding individuals with missing data in more than three loci (54 individuals excluded out of 286). Based on this dataset, a final analysis was performed excluding all individuals of *M. bouvieri*, a species not expected to hybridize with any of the other ones because of the morphological and behavioral differences.

2.4. COI

For COI amplification, the primers LCO1490 (Folmer et al., 1994) and PatMessor (Steiner et al., 2011) were used. In the case of PCR or sequencing failure, the primer Jerry C1-J-2183f (Simon et al., 1994) was used instead of PatMessor.

PCRs were conducted in 10 µl reaction volume containing 1× RotorGene Probe PCR Kit, 0.2 µM forward and reverse primers, and 1 µl template DNA. PCR conditions were an initial denaturation step at 95 °C

Table 3
Microsatellite primers for *Messor*. Primer ID, template DNA (μl), annealing temperature (°C), cycle number, label, mix, and number of alleles.

Primer ID	Template DNA (μl)	Annealing temp. (°C)	Cycle number	Label	Mix	Number of alleles
Mmap011	0.5	50	32	FAM	1	4
Mmap057	0.5	50	32	HEX	1	11
Mmap060	0.5	50	32	NED	1	5
Mmap071	0.5	55	32	PET	1	16
Mmap086	0.5	55	32	FAM	2	11
Mmap091	1	51	40	NED	2	17
Mmap120	0.5	50	32	PET	2	18
Mmap144	1	51	40	NED	4	15
Mmap148	1	51	40	NED	3	19
Ms24B	0.5	50	32	FAM	3	9
Ms13J	0.5	55	32	PET	3	12
Ms1A	0.5	50	32	FAM	4	15
Ms2A	0.5	50	32	HEX	2	11
Ms2C	0.5	50	32	HEX	3	14
Ms2D	0.5	55	32	PET	4	9

for 3 min, 35 cycles with 95 °C for 30 s, 50 °C for 45 s, and 72 °C for 2 min, and a final extension step at 72 °C for 10 min. PCR success was controlled by agarose gel electrophoresis. PCR products were incubated with 20 U Exo1 and 1 U FastAP. Sanger sequencing in both directions was performed by Eurofins GmbH (Ebersberg, Germany) using the same primers as for the PCR.

COI sequencing was successful in 252 workers (one to eight per colony; on average, 4.3 ± 3.1 standard deviation). Sequences were visualized with Chromas v.2.6 (McCarthy 1996), edited and deposited at GenBank (accession numbers MT407660-MT407889, GenBank Submission SUB7341713), and aligned with ClustalX v.2.0.12 (Thompson et al., 1997). The final size of the alignment was 1189 base pairs. *Aphaenogaster iberica* Emery, 1908, *Messor lobognathus* Andrews, 1916, and *Messor chamberlini* Wheeler, 1915 (GenBank accession numbers DQ074361-DQ074363) were used as outgroups (cf. Steiner et al., 2011).

Phylogenetic analyses were conducted with MEGA v.7.0.26 (Kumar et al., 2016). Three trees were generated: a Neighbor-Joining tree (Saitou and Nei 1987; Nei and Kumar 2000) using the Kimura 2-parameter model, a Maximum Parsimony tree, and a Maximum Likelihood tree (Nei and Kumar 2000) using the General Time Reversible model with Gamma distributed and Invariant sites (GTR + G + I), as indicated by the BIC values of a Model Selection analysis. Pairwise distances between and within groups were calculated with a Distance Estimation analysis using the Kimura 2-parameter model. For each tree and the Distance Estimation analysis, the number of bootstrap replications was 1000 (Felsenstein 1985). Bayesian Inference (BI) was generated with MrBayes v.3.2.7a (Ronquist et al., 2012). The GTR+G+I model was used for two parallel runs with four Markov chains each for 20,000,000 generations, and a tree was recorded every 5000 generations. The length of burnin period was set 2500 as the standard deviation of split frequencies was below 0.01 after 12,500,000 generations.

A search with the Basic Local Alignment Search Tool (BLAST; Altschul et al., 1990) was conducted to compare the sequences obtained in this study with those in GenBank. An additional alignment with ClustalX v.2.0.12 (Thompson et al., 1997) was done between the *M. barbarus* sequences of two different subclades with those of Romiguier et al. (2017) available via the Short sequence archive of GenBank (accession numbers SRR1325007-SRR1325016, SRR4292909, SRR4292920, SRR4292931, SRR4292934-SRR4292904).

2.5. Morphometrics

Morphometric measurements were taken from every individual that was successfully amplified in both genetic methods. Altogether, 16 continuous morphometric traits (Table 4, Fig. 2) were measured on 216 workers representing 34 nest samples (three to eight per colony; on average, 5.7 ± 1.4 standard deviation) from the focal study area and additional sites and further 24 singletons collected from the focal study area. The material is deposited in the Hungarian Natural History Museum Budapest, the National Museum of Natural History Paris, the National Museum of Natural Sciences Madrid, the Natural History Museum Basel, the Natural History Museum Vienna, and the private collection of Sándor Csősz. The full list of material investigated is given in Table S1.

2.5.1. Morphometric character recording protocol

Morphometric characters were defined based on Seifert (2018). All measurements were made in μm using a pin-holding stage, permitting rotations around X, Y, and Z axes. An Olympus SZX9 stereomicroscope was used at a maximum magnification of 150×; if a character was larger than the ocular field, smaller magnification was applied. Morphometric data are provided in μm throughout the whole paper. All worker individuals were measured by SC. Definitions of morphometric characters are given in Table 4. For broader details, see Seifert (2018).

2.5.2. Statistical framework on morphometric data – hypothesis formation and testing

2.5.2.1. Exploratory analyses through NC clustering and PART. For all

Table 4
Abbreviations (Abbr.) of morphometric characters and definition of measurements.

Abbr.	Definition of measurements
CL	Maximum median length of head capsule. The head must be carefully tilted so the maximum length is positioned in the measuring plane.
CW	Maximum head with including compound eyes. The largest distance between profiles of the two compound eyes in full-face view.
POC	Post ocular distance. Use a cross-scaled ocular micrometer and adjust the head to the measuring position of CL. Caudal measuring point: median occipital margin; frontal measuring point: median head at the level of the posterior eye margin
EL	Eye length. Maximum diameter of the compound eye.
FR	Minimum distance of the frontal carinae.
FL	Maximum distance of frontal carinae.
AnScD	Torular lamellae distance. Distance between distalmost edges of torular lamellae.
ML	Diagonal length of the alitrunk in profile. Measured in lateral view from the anteriormost point of anterior pronotal slope to the caudalmost point of the lateral metapleural lobe.
MW	Maximum width of pronotum.
NOL	Petiole node length; measured in lateral view, from the center of the petiolar spiracle to the posterior profile.
PeW	Petiole width. The maximum width of petiole in dorsal view.
MpDep	Mesopropodeal depression depth. Measured in lateral view, from a reference line set ont he highest profile of propodeum and pronotum, or mesonotum to the deepest point of the depression.
SL	Scape length. The maximum straight-line scape length excluding the articular condyle.
HTL	Hind tibia length. Measured from the distalmost point of the tibia to the proximal end where the tibia is narrowest in profile.
ScBW	Maximum distance of the anterior corner at scape base from the anterior surface of the condlyrar neck.
ScBaC	Maximum distance between the corners at scape base.
PrOC	Malar distance. It is the shortest distance between the anteriormost margin of the compound eye and the closest margin of head capsle by the mandibular joint.

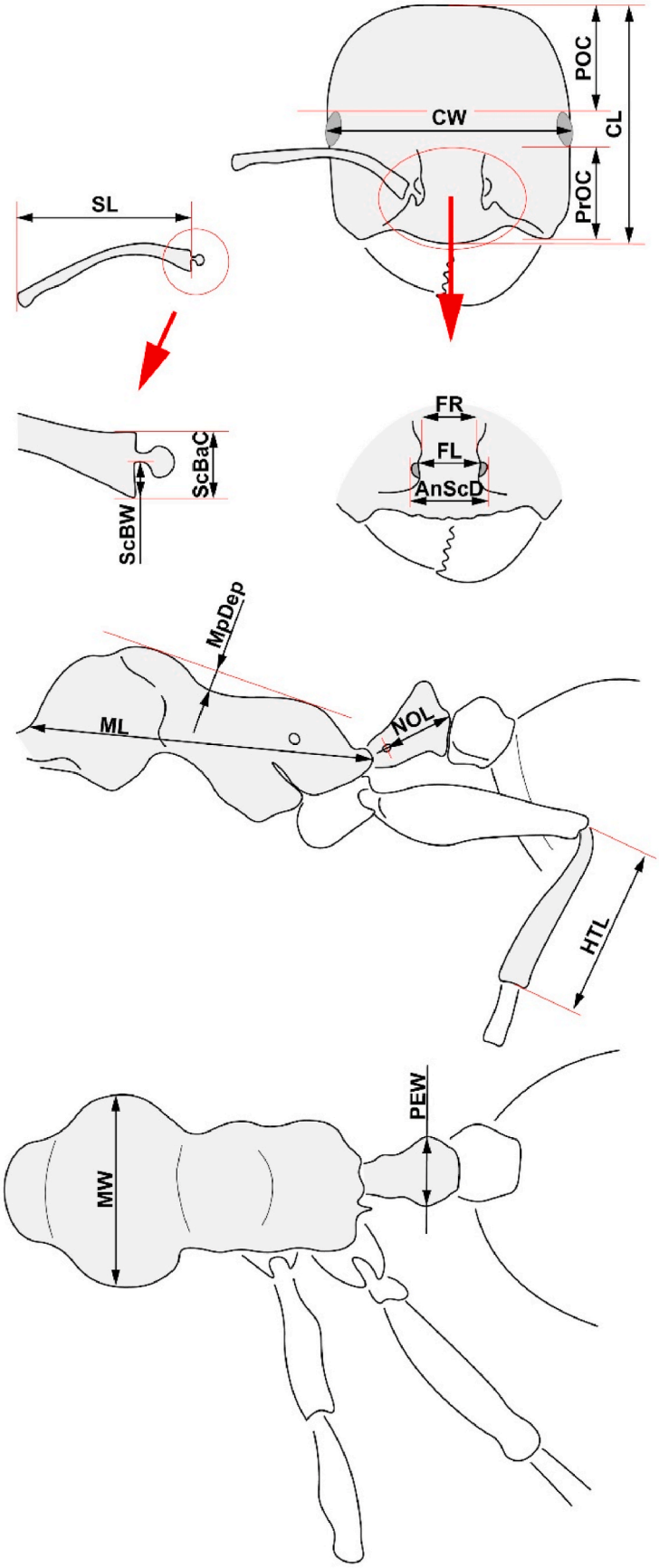

Fig. 2. Position of morphometric characters on head in frontal view, including scape and frontal triangle, and on mesosoma in lateral and dorsal view; see Table 4 for definition of abbreviations and measurement of characters.

workers analyzed morphometrically, a prior species hypothesis was generated from all the 16 morphometric variables through NC clustering (Seifert et al., 2014). NC clustering searches for discontinuities in morphometric data and sorts all similar cases into subsets in a two-step process. The first step reduces dimensionality in the data via cumulative linear discriminant analysis (LDA) using nest samples as groups (Seifert et al., 2014). The second step calculates pairwise Euclidean distances between samples using LD scores as input and displays the distance matrix in a dendrogram. The NC-clustering was done via the packages *cluster* (Maechler et al., 2014) and *MASS* (Venables and Ripley 2002) in R version 4.0.2 (R Development Core Team, 2020). The ideal number of clusters was determined by Partitioning Algorithm based on Recursive Thresholding via the package clusterGenomics (Nilsen and Lingjaerde, 2013). The method estimates the number of clusters in data based on the recursive application of the Gap statistic (Tibshirani et al., 2001) and can discover both top-level clusters and sub-clusters nested within the main clusters. The script for NC-clustering combined with PART was written in R and can be found in Appendix S1 in Csősz and Fisher (2016). Our exploratory data analysis approach follows the protocol described by Csősz and Fisher (2016) with the following specific settings: bootstrap iterations in PART were set to 'b = 1000', and the minimum size of clusters was set to 'minSize = 5' for both 'hclust' and 'kmeans'. The optimal number of clusters and the partitioning of samples were accepted as the prior species hypothesis in every case in which the two clustering methods, 'hclust' and 'kmeans' through PART, yielded the same conclusion.

2.5.2.2. Hypothesis testing by confirmatory analyses. The validity of the prior species hypothesis was tested via Linear Discriminant Analysis (LDA) using the package *MASS*. Classification hypotheses were imposed for all samples that were congruently classified by partitioning methods, while wild-card settings (i.e. no prior species hypothesis imposed on its classification) were given to samples that were incongruently classified by the two partitioning methods. Statistical analyses were done in R.

2.6. Species concept, species delimitation criteria, and consideration of described taxa

The Unified Species Concept (Queiroz 2007) was applied, which defines a separately evolving metapopulation lineage as the only necessary conceptual property of species. The species delimitation criteria used were: microsatellites – genotypic clusters (Mallet 1995) for the STRUCTURE results; mtDNA – reciprocal monophyly (Donoghue 1985) for the phylogenetic trees; morphometrics – a gap statistic (Tibshirani et al., 2001) employed to identify discontinuities in the data.

To avoid describing a species identical to an already existing taxon, all relevant *M. barbarus/capitatus* group taxa from the West Mediterranean region were studied, including Europe and the Western part of North Africa, in antweb.org (as of 12 July 2023). Also, all valid taxon names from the given territory in Bolton (2022) were considered.

3. Results

3.1. Microsatellites

All 286 workers, 94 from the focal study area and 192 from the additional sites (for details, see Table S1), were successfully microsatellite-genotyped in at least one up to all 15 loci. The numbers of genotyped workers were 78 for the unidentified *Messor*, 72 each for *M. barbarus* and *M. bouvieri*, and 64 for *M. capitatus*. In the Linkage Disequilibrium test, out of 105 possible combinations of loci, there was linkage 12 times in *M. barbarus*, two times in *M. bouvieri*, 21 times in *M. capitatus*, and four times in the unidentified *Messor*. The five most frequently linked loci were Ms13J, Mmap057, Mmap060, Ms2C, and Ms2D (Table S2), which were excluded in a further STRUCTURE analysis (see 2.3 Microsatellites). There were many deviations from Hardy–Weinberg Equilibrium (Table S3). The number of allele frequencies per locus was highest with 19 and lowest with 4 (Table 3). The total number of alleles was 186.

In the Bayesian cluster analysis, K = 4 was indicated as the most probable number of clusters (Fig. 3). For this K, the samples of the unidentified *Messor* were classified in a separate cluster and each of the three species *M. barbarus*, *M. bouvieri*, and *M. capitatus* formed one of the other three clusters (Fig. 4). The results were the same in the additional analyses done after excluding loci and individuals (see 2.3. Microsatellites).

3.2. COI

252 workers were successfully COI-sequenced, 91 from the focal study area and 161 from the additional sites (for details, see Table S1). The numbers of successfully COI-sequenced workers per species were 76 for the unidentified *Messor*, 68 for *M. barbarus*, 59 for *M. bouvieri*, and 49 for *M. capitatus*. All phylogenetic methods applied on the data returned highly congruent tree topologies. The samples of the unidentified *Messor* formed a separate clade, and each of the three species, *M. barbarus*, *M. bouvieri*, and *M. capitatus*, formed one of the other three monophyletic clades. The clade of *M. barbarus* contained two subclades, which were not geographically separated. Each clade and subclade were clearly supported by the bootstrap replications (Neighbor Joining: Fig. 5;

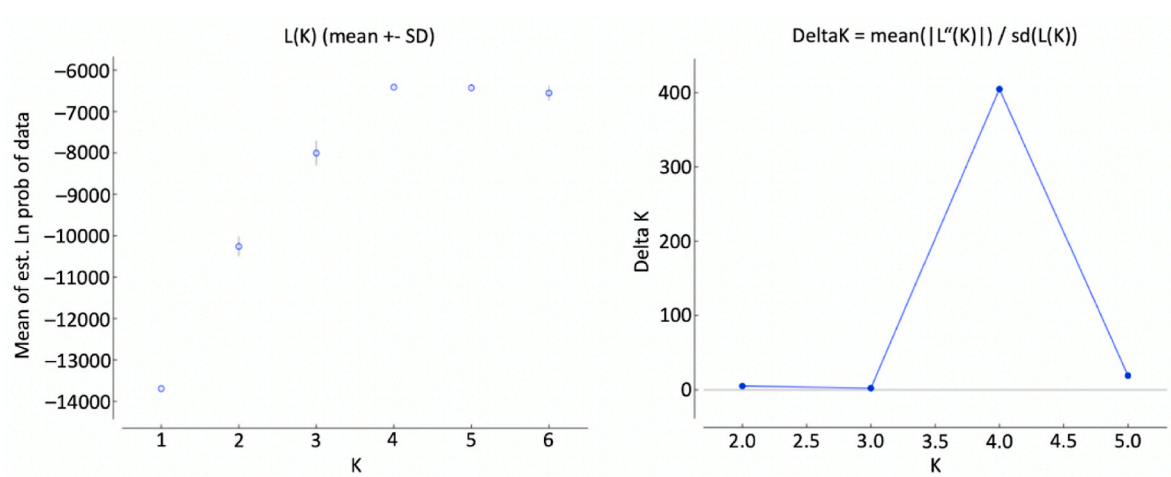

Fig. 3. Method of Evanno et al. (2005) implemented on the STRUCTURE output data. L(K): mean ± standard deviation (SD) (left) and DeltaK (right). The analysis was conducted in STRUCTURE Harvester (Earl and von Holdt 2012).

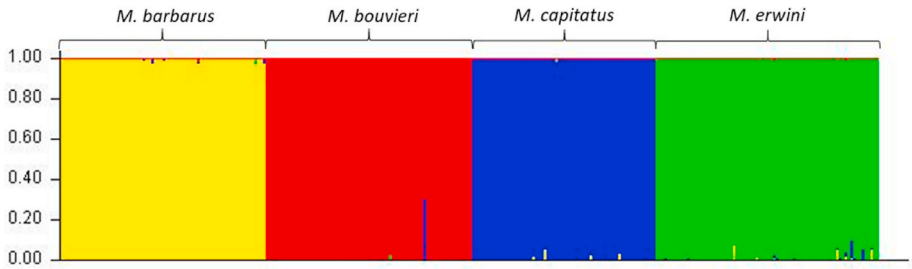

Fig. 4. Bar plot of the Bayesian cluster analysis based on microsatellites genotyped in 286 individuals. The number of clusters is 4: *Messor barbarus* (yellow cluster), *M. bouvieri* (red), *M. capitatus* (blue), and the hitherto unidentified *M. erwini* sp. n. (green). The y axis shows the percentage of assignment to a certain cluster. The analysis was conducted in STRUCTURE 2.3.4 (Pritchard et al., 2000).

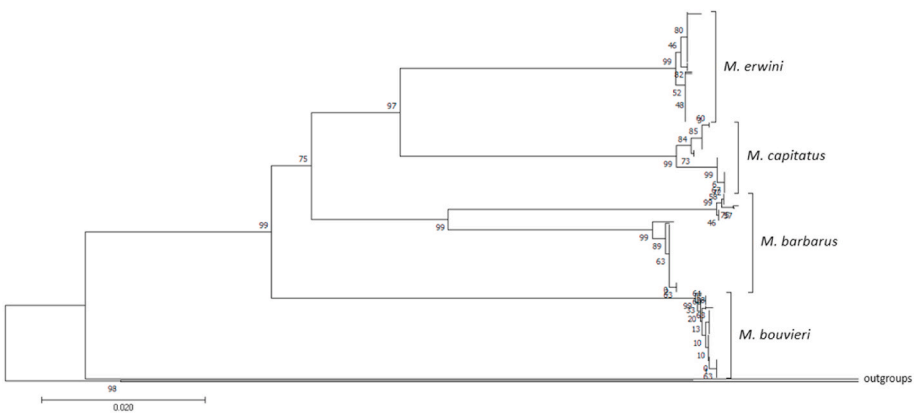

Fig. 5. Phylogenetic analysis based on COI of *Messor barbarus*, *M. bouvieri*, *M. capitatus*, and the hitherto unidentified *M. erwini* sp. n. with *Aphaenogaster iberica*, *M. lobognathus*, and *M. chamberlini* as outgroups, using the Neighbor-Joining method based on Kimura 2-parameter. The percentage of replicate trees in which the associated taxa clustered together in the bootstrap test (1000 replicates) are shown next to the branches. The analysis was conducted in MEGA 7.0.26 (Felsenstein 1985; Saitou and Nei 1987; Nei and Kumar 2000; Kumar et al., 2016).

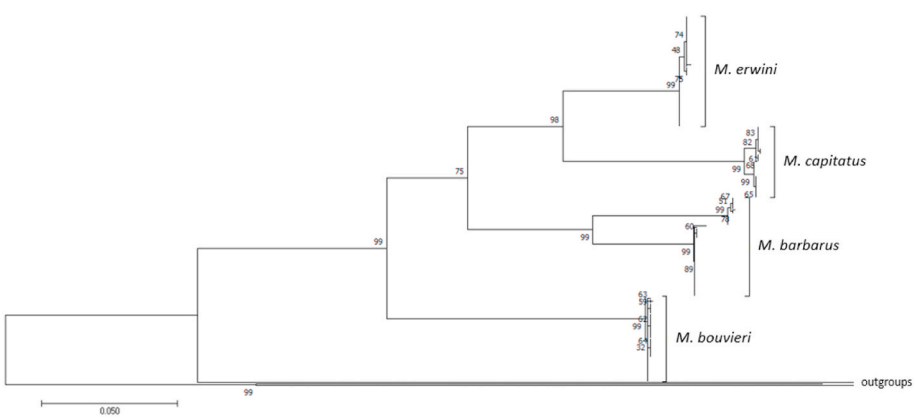

Fig. 6. Phylogenetic analysis based on COI of *Messor barbarus*, *M. bouvieri*, *M. capitatus*, and the hitherto unidentified *M. erwini* sp. n. with *Aphaenogaster iberica*, *M. lobognathus*, and *M. chamberlini* as outgroups, using the Maximum Likelihood method based on the General Time Reversible model. The percentage of replicate trees in which the associated taxa clustered together in the bootstrap test (1000 replicates) are shown next to the branches. The analysis was conducted in MEGA 7.0.26 (Nei and Kumar 2000; Kumar et al., 2016).

Table 5
Pairwise distances (Kimura 2-parameter model) between the two subclades *Messor barbarus* 1 and 2, the four clades *M. barbarus* (subclades 1 and 2 as defined by Romiguier et al., 2017), *M. bouvieri*, *M. capitatus*, the hitherto unidentified *M. erwini* sp. n., and the outgroups. The distances were calculated in MEGA 7.0.26.

Distance (%)	*M. barbarus* 1	*M. barbarus* 2	*M. barbarus* (1 + 2)	*M. bouvieri*	*M. capitatus*	*M. erwini*
M. barbarus 1						
M. barbarus 2	6.0					
M. bouvieri	10.5	10.5	10.5			
M. capitatus	10.1	9.2	9.5	10.5		
M. erwini	9.6	9.1	9.2	10.6	7.4	
Outgroups	17.8	17.4	17.5	17.8	17.8	17.5

Maximum Likelihood: Fig. 6; Maximum Parsimony: Fig. S1; Bayesian Inference: Fig. S2). Based on pairwise distance calculations using the Kimura 2-parameter model, the distance from the unidentified *Messor* was lowest to *M. capitatus* (7.4%) and highest to *M. bouvieri* (10.6%). The distance between the two subclades of *M. barbarus* was 6.0% (Table 5). The intraspecific distance was highest with 2.5% in *M. barbarus*, while it was 0.5% in *M. capitatus* and 0.1% in both *M. bouvieri* and the unidentified *Messor*.

The sequences of the unidentified *Messor* resembled most the GenBank sequences of *M. capitatus* with 93.4% accordance (checked in

January 2020; GenBank accession DQ074359.1). In the additional alignment (see 2.4. COI), the two *M. barbarus* subclades were equivalent to the two lineages discovered by Romiguier et al. (2017).

3.3. Morphometrics

In total, 216 workers were analyzed morphometrically, 75 from the focal study area and 141 from the additional sites (for details, see Table S1). The numbers of morphometrically analyzed workers per species were 59 for the unidentified *Messor*, 55 for *M. barbarus*, 57 for *M. bouvieri*, and 45 for *M. capitatus*. The exploratory analysis (NC-PART clustering) run on the 189 worker individuals from 34 nest samples that were successfully amplified in both genetic analyzes returned four separate clusters; this pattern was identically returned by both partitioning clustering algorithms, 'hclust' and 'kmeans' (Fig. 7). The clusters were also corroborated by the confirmatory LDA, yielding a single misclassification out of the total 191 individuals. The classification success was 99.5%. The 22 additional singletons from the overlapping geographic area were analyzed as wildcards (i.e., no grouping hypotheses were imposed for these cases) in LDA. Only two out of these 22 (error rate: 9.1%) worker individuals got an alternative clustering hypothesis compared with the molecular findings.

4. Discussion

The aim of the study was to characterize the unidentified *Messor* colonies from a Catalonian site. An integrative approach was used, combining microsatellites, COI, and morphometrics. All species delimitation criteria, the genotypic clusters for the STRUCTURE results, the reciprocal monophyly for the phylogenetic trees, and the gap statistic for the morphometrics, confirm the unidentified *Messor* as an entity clearly separated from *M. barbarus*, *M. bouvieri*, and *M. capitatus* (Figs. 4–7). Thus, applying the Unified Species Concept (Queiroz 2007), the hitherto unidentified *Messor* population represents a separate species, which is described as *M. erwini* sp. n. hereby (Section 5.). Hereafter, we discuss the results in the light of the three hypotheses presented in the introduction.

(i) Cryptic speciation: Under this hypothesis, the unidentified *Messor* colonies form a separate species. This hypothesis is supported by the results of the morphometric analysis and of both genetic methods. In the NC-PART clustering analysis (Fig. 7) as well as in the Bayesian cluster analysis (Fig. 4), the unidentified *Messor* is assigned to a separate cluster, as each of the three other species analyzed, which indicates four separate species. The indication of separate species through Bayesian cluster analyses is corroborated by other STRUCTURE analyses in *Messor* (Steiner et al., 2011), in *Formica* Linnaeus, 1758 (Bernasconi et al., 2011), and in *Camponotus* Mayr, 1861 (Ronque et al., 2016), which also resulted in separate species forming separate clusters. Bayesian clustering results can be influenced by linked loci, missing data, uneven allele frequency distributions, and uneven sample sizes (Kalinowski 2011; Puechmaille 2016), but such a distortion of our results is very implausible, as the clusters are the same across all additional analyses with modified datasets. The hypothesis of a cryptic species is also supported by the phylogenetic analyses, as in all of them the unidentified *Messor* samples form a separate clade, distinct from the other species (Figs. 5 and 6). Similarly, in the multidisciplinary approach of Steiner et al. (2018), four of the five revealed *Messor* species formed separate clades in the phylogenetic tree as well. Only one species formed three subclades, but these did not show separations in the other disciplines of the study (Steiner et al., 2018). This is comparable with the two subclades of *M. barbarus* that we retrieved and that are equivalent to those found by Romiguier et al. (2017), which also were not separated in the Bayesian cluster analysis. Our results as well are in agreement with studies in other genera such as in *Solenopsis* Westwood, 1840 (Ross et al., 2010; Chialvo et al., 2018) and in *Cataglyphis* Foerster, 1850 (Eyer et al., 2017; Eyer and Hefetz 2018), which also suggested distinct species by detecting separations in both the Bayesian cluster analysis and the phylogenetic trees. In the latter study, the cryptic species partially co-occurs with other species of this genus as well (cf. Eyer and Hefetz 2018). The coexistence of genetically distinct populations in the same local area provides strong evidence for reproductive isolation and thus again for separated species (Koffi et al., 2010; cf. Chialvo et al., 2018).

(ii) Hybridization between *M. barbarus* and *M. capitatus*: The samples of the unidentified *Messor* are not hybrids, as they form separate clusters in the NC-PART clustering analysis and the Bayesian

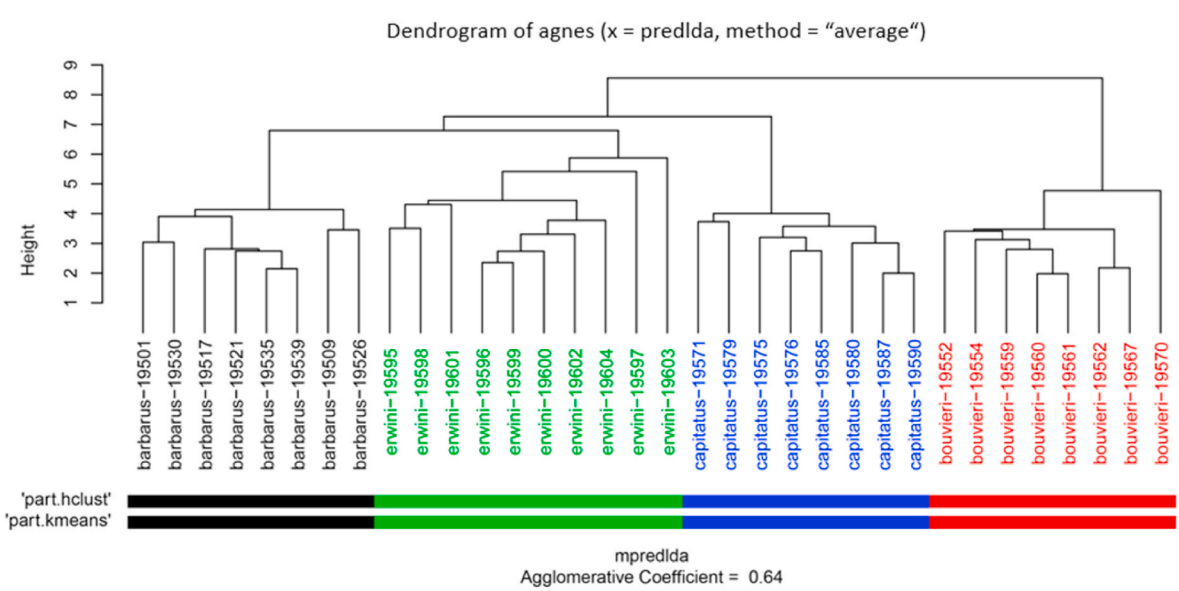

Fig. 7. Dendrogram solution for the morphometric data of Iberian *Messor* species. Sample information in the dendrogram given as follows: final species hypothesis followed by a five-digit sample code applied by the genetic lab separated by a hyphen. Two columns of rectangles represent results of the partitioning algorithms 'hclust' and 'kmeans'. Different colors distinguish species. *Messor barbarus*: black, *M. erwini* sp. n.: green, *M. capitatus*: blue, *M. bouvieri*: red.

Table 6
Consideration of all relevant *M. barbarus/capitatus* group taxa from the West Mediterranean region including Europe and the Western part of North Africa, in antweb.org (retrieved on 12 July 2023) and of all valid taxon names from the given territory in Bolton (2022) as well as resulting diagnosis and conclusion. Source studied: specimen ID in antweb.org or reference to original description.

Taxon name	Source studied	Locality	Diagnosis	Conclusion
M. barbarus nigriceps	CASENT0913162	Spain: Cáceres	psammophore absent, propodeum rounded in profile	junior synonym of *M. barbarus*
Messor barbarus capitatus grandiceps [quadrinomial]	FOCOL1249	Spain: Cádiz	psammophore absent, propodeum angulate in profile, frontal triangle smooth	*M. capitatus*
Messor celiae Reyes, 1985	original description	Spain: Cordoba	petiole lamelliform, extremely high	out of the target complex
Messor hispanicus Santschi, 1919	CASENT0913187	Spain: Pozuelo de Calatrava	coarsely sculptured body	out of the target complex
Messor ibericus Santschi, 1931	CASENT0904129	null	coarsely sculptured body	member of *M. structor* complex
Messor lobicornis (Forel, 1894)	CASENT0907750	Algeria: Terni	coarsely sculptured body	out of the target complex
Messor lusitanicus Tinaut, 1985	CASENT0900470	"Portugal"	psammophore present, head microreticulate, propodeal denticle well-developed	out of the target complex
Messor lobicornis batnensis Forel, 1909	CASENT0907751	Algeria: Batna	head coarsely microreticulate, dull; propodeal spines very long	out of the target complex
Messor marocanus Santschi, 1927	CASENT0281606	Morocco: Mogador	psammophore absent, propodeum angulate in profile, frontal triangle costulate; D3 = -2.97 which is much lower than that of *M. erwini*: +2.795 [+0.625, +5.063]	*M. capitatus/barbarus* complex species
Messor minor hesperius Santschi, 1927	CASENT0913204 (major) and CASENT0913205 (minor)	Spain: Tenerife, Médano	psammophore absent, propodeum angulate in profile, frontal triangle costulate; D3 = +2.437 and −3.922; the latter is far below the D3 range of *M. erwini*.	*M. capitatus/barbarus* complex species; the synonymy with *M. erwini* rejected based on the partially outlying D3 scores
Messor sordidus (Forel, 1892)	CASENT0907738	Spain: Andalusia	psammophore absent, propodeum rounded in profile	*M. capitatus/barbarus* complex species
Messor timidus Espadaler, 1997	CASENT0915456	Spain: Almería, Sartenilla	psammophore present, head microreticulate, propodeal denticle well-developed	out of the target complex

cluster analysis and separate clades in the phylogenetic analyses (Figs. 4–7). To compare, the hybrids between *M. minor* and *M.* cf. *wasmanni* detected by Steiner et al. (2011) were morphometrically identified as intermediates between these species, and they were assigned to the clusters and clades of the two pure species in the Bayesian cluster analysis and in the phylogenetic analyses, respectively, instead of forming separate ones (cf. Steiner et al., 2011). Like the *Messor* hybrids, the same assignments to the clusters and clades of the pure species showed hybrids between *Tetramorium caespitum* (Linnaeus, 1758) and *Tetramorium immigrans* Santschi, 1927 (Cordonnier et al., 2019).

(iii) Social hybridogenesis: Romiguier et al. (2017) characterized this reproduction mode for Spanish *M. barbarus*: There are two lineages of this species (included also in our study: Figs. 1, 5 and 6). Queens mating with males of their own lineage produce sexuals, and queens mating with males of the other lineage produce workers. Concerning our data, under this hypothesis, we would expect two COI lineages (of which at least one is represented by the unidentified *Messor* samples) contributing to a single cluster in the Bayesian cluster analysis of the microsatellite data given that workers were analyzed (for sexuals, two separate microsatellite-based clusters would be expected, and the workers would then be classified as admixed between the two). We did not detect such pattern in our data. However, we cannot exclude that social hybridogenesis occurs within the new, hitherto cryptic *Messor* species, as a slight but not supported differentiation into two COI lineages can be discerned in Fig. 5; the existence of such hybridogenesis would, however, not bear on our conclusion of a new species.

As in the phylogenetic analyses, *M. capitatus* was the most resembling species when searching sequences of the unidentified *Messor* in GenBank (checked in January 2020), while the corresponding species was not yet registered there. The species was neither morphologically described before as our consideration of described taxa based on antweb.org (retrieved on 12 July 2023) and Bolton (2022) revealed (Table 6); in some previous studies, it was reported as "*M. capitatus*" (e.g., Arnan et al., 2010; Arnan et al., 2012).

Messor erwini sp. n. could have emerged through recent divergence or through stasis, as the sympatric species are closely related, and their morphological similarities are high (cf. Struck et al., 2018); in-depth analysis would be needed to solve this question (cf. Wagner et al., 2018). The exceptional local co-occurrence of the three species with high colony densities can be explained by ecological niche theory, as the heterogenous habitat provides potential for different ecological niches. Possible explanations could be differences in the size of seeds collected by the species (cf. Cerdá and Retana 1994) or in their foraging behavior (Cerdá and Retana 1994; Arnan et al., 2010; Plowes et al., 2013; X. Arnan and R. Pol, unpublished).

In conclusion, our study confirms a separate species of *Messor* in Catalonia, which has been neither genetically nor morphologically described before. However, its distribution for now seems to be very narrow, as the colonies of *M. erwini* sp. n. have been detected in just one study site. Aims for future research on this newly discovered species thus include screening of Mediterranean habitats comparable with the type

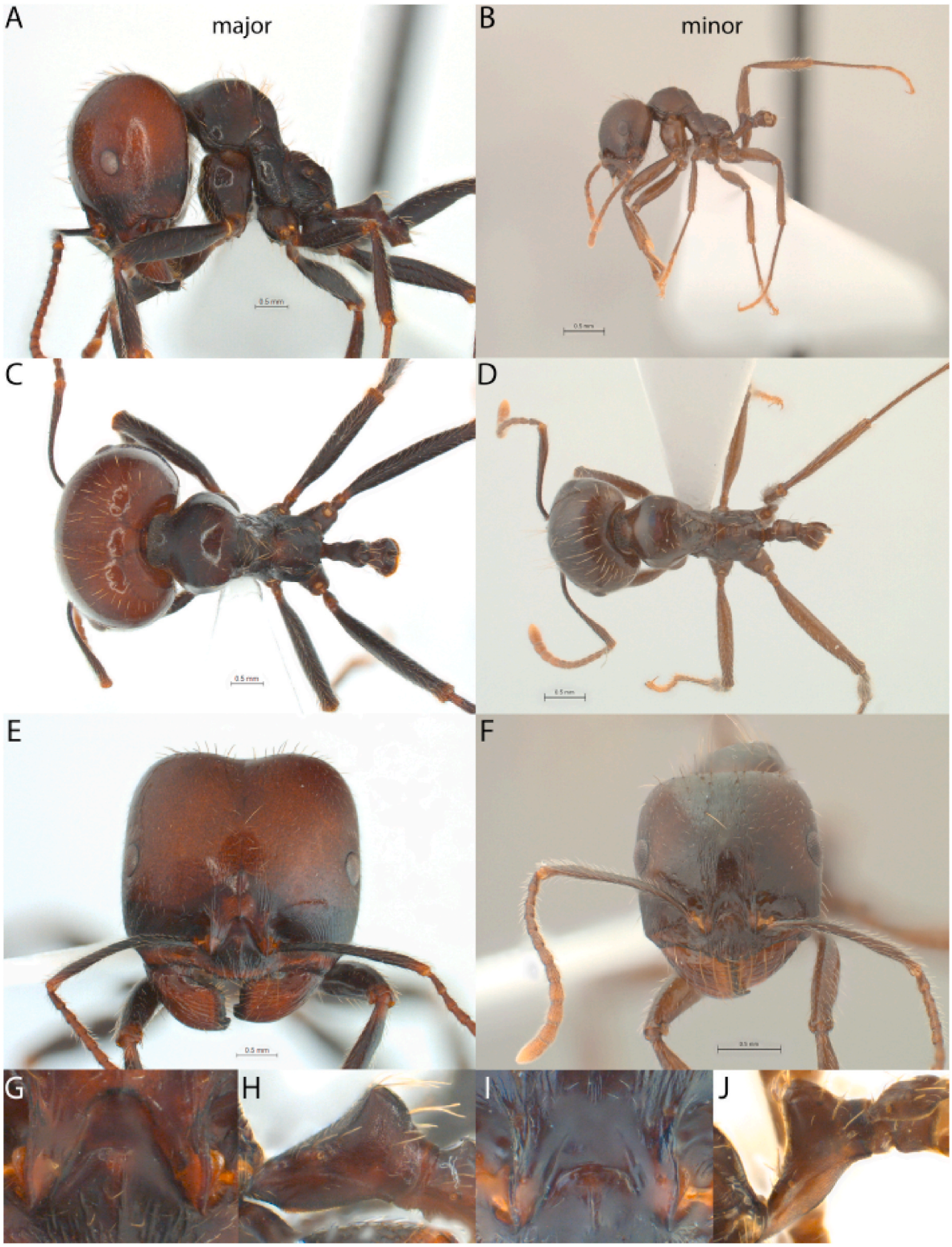

Fig. 8. *Messor barbarus* major (A, C, E, G, H; collection code #19610) and minor (B, D, F, I, J; collection code #19612) workers. Lateral view of body (A, B); dorsal view of body (C, D); head in full-face view (E, F); frontal triangle in larger magnification (G, I); lateral view of petiole in larger magnification (H, J).

location as well as analysis of additional morphological characters (e.g., on the gaster, which was not available here due to DNA extraction) and more detailed analysis of the ecological and behavioural niche. A new species in *Messor* raises the question if there are even more than the about 10 already known species in Spain. Then, a broader diversity in *Messor* also can be assumed from a global view.

5. Taxonomic key and formal descriptions

(Fig. 8A–J, 9A-J, 10A-J, 11A-J)

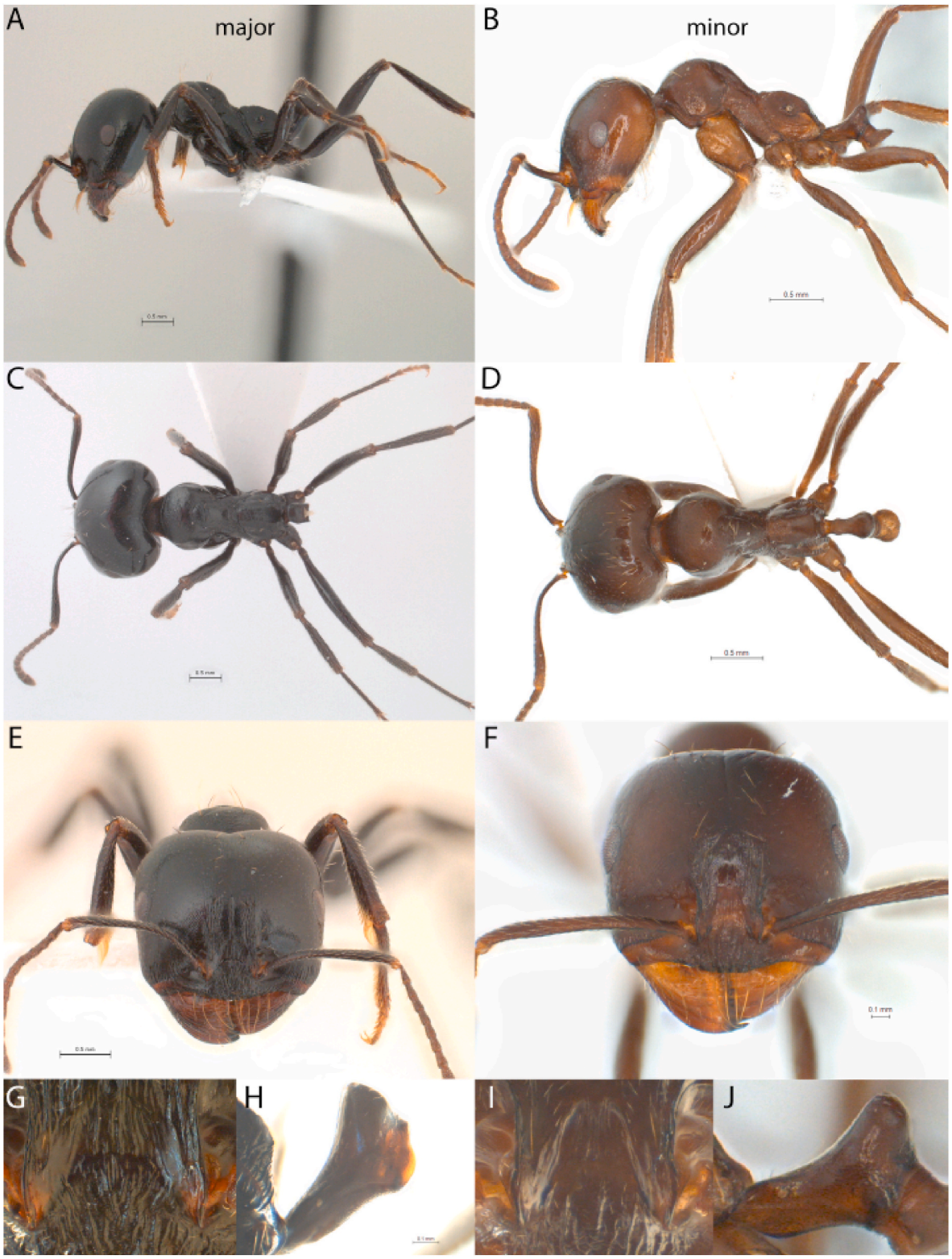

Fig. 9. *Messor bouvieri* major (A, C, E, G, H; collection code #19624) and minor (B, D, F, I, J; collection code #19620) workers. Lateral view of body (A, B); dorsal view of body (C, D); head in full-face view (E, F); frontal triangle in larger magnification (G, I); lateral view of petiole in larger magnification (H, J).

5.1. Key to workers

1 Psammophore, i.e., numerous long, J-shaped hairs, posterior to buccal cavity, present (Fig. 9A and B). Only pubescent hairs present on petiolar node dorsum, long dorsal setae absent (Fig. 9H, J). A few standings hairs present on the sides of peduncle, which are no longer than 100 µm (40–80 um). Basal scape lobe weekly developed (ScBaC/CS mean 0.031 [0.025, 0.036]) … ***M. bouvieri***

- Psammophore posterior to buccal cavity absent, only C-shaped, or strait hairs present (Fig. 8A and B; Fig. 10A and B; Fig. 11A and B). Long, standing hairs present on the dorsum of petiolar node (Fig. 8H, J; Fig. 10H, J; Fig. 11H, J). The longest hairs are longer than 200 µm

Fig. 10. *Messor capitatus* major (A, C, E, G, H; collection code #19646) and minor (B, D, F, I, J; collection code #19643) workers. Lateral view of body (A, B); dorsal view of body (C, D); head in full-face view (E, F); frontal triangle in larger magnification (G, I); lateral view of petiole in larger magnification (H, J).

(200–400 um). Basal scape lobe well developed (ScBaC/CS 0.050 [0.032, 0.063]), having an acute projection externally … **2**

2 Minor workers: mesonotum and propodeum smooth and shiny or with inconspicuous transversal rugae (Fig. 8B, D); Major workers: propodeum rounded in profile. mesonotum and propodeum parallelly rugulose, sides of pronotum feebly rugulose, ground surface smooth and shagreened (Fig. 8A, C) … ***M. barbarus***

- Minor workers: mesonotum and propodeum with conspicuous, or coarse transversal rugae (Fig. 10B, D; Fig. 11B, D); Major workers: propodeum angulate in profile or bear a pair of propodeal tubercles, which are dentiform or lamelliform in the largest workers.

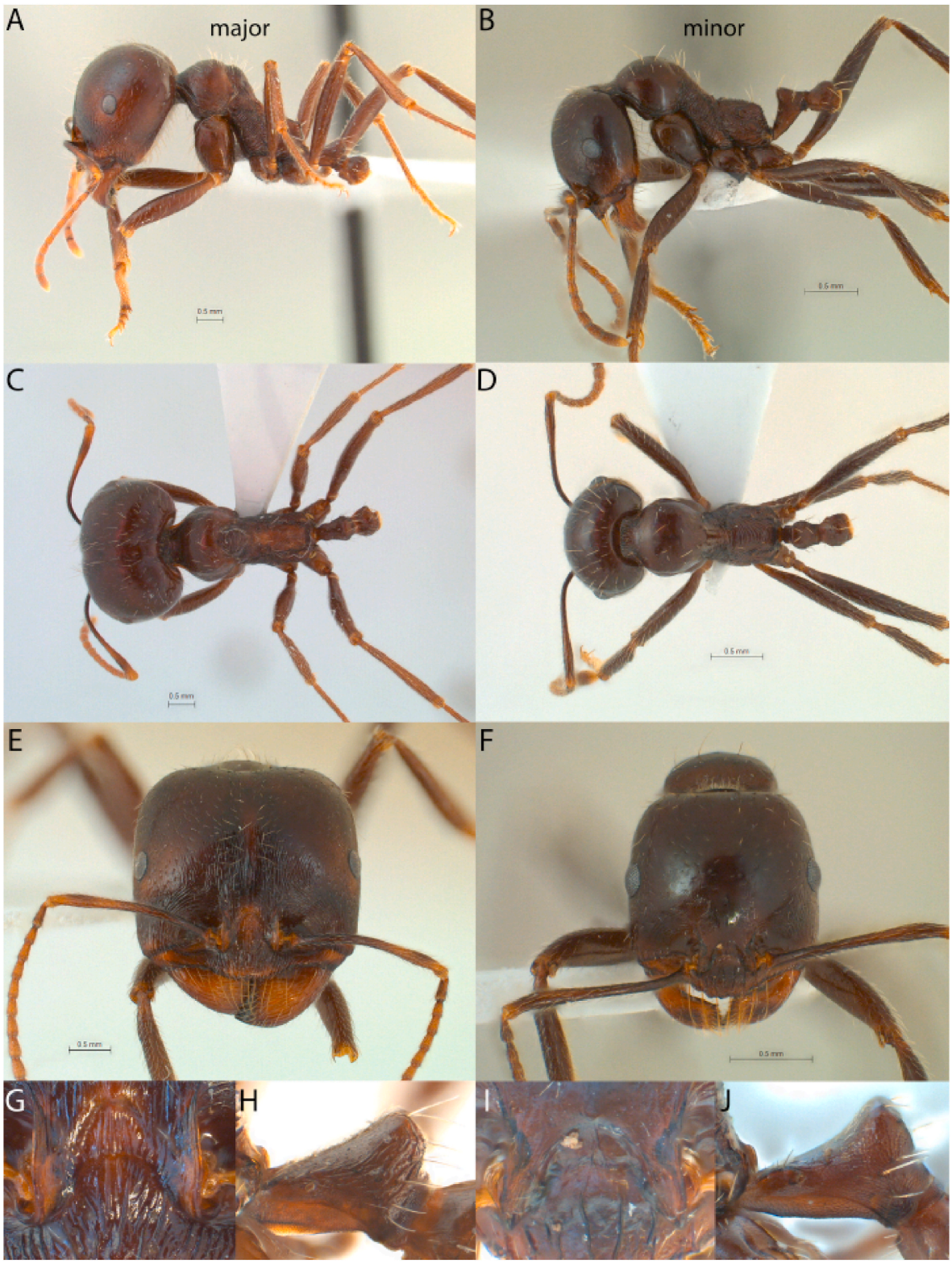

Fig. 11. *Messor erwini* sp. n. major (A, C, E, G, H; holotype; collection code #19603e) and minor (B, D, F, I, J; paratype; collection code #19603d) workers. Lateral view of body (A, B); dorsal view of body (C, D); head in full-face view (E, F); frontal triangle in larger magnification (G, I); lateral view of petiole in larger magnification (H, J).

Mesonotum and propodeum parallelly rugose, sides of pronotum rugose (Fig. 10A, C; Fig. 11A, C) … **3**

3 The frontal triangle inconspicuously sculptured (Fig. 10G, I); surface smooth, shagreened, or irregularly striate. Median clypeal costa does not run across the frontal triangle. The largest major workers have dentiform propodeal tubercles (Fig. 10A). Using the following combination of three numeric characters is advisable for reliably telling species of this couplet apart: D3 = 0.078 ×FL -0.107 ×AnScD +0.021 ×SL -8.123. This numeric key yields 100% of classification success in

case of each subcaste. D3 is in the negative range, mean = −2.078 [-3.939, −0.253] (n = 45) … ***M. capitatus***

- The frontal triangle conspicuously sculptured (Fig. 11G, I); surface shagreened or irregularly striate. At least the well-developed median clypeal costa runs across the frontal triangle from the base to the apex. In major workers often more costae present on the frontal triangle. The largest major workers have lamelliform propodeal tubercles (Fig. 11A). D3 is in the positive range, mean = +2.795 [+0.625, +5.063] (n = 50) … ***M. erwini* sp. n.**

5.2. Formal descriptions of Iberian Messor species (alphabetic order)

5.2.1. Messor barbarus

(Fig. 8A–J, Table S1, Table 7)

Relatively large species; Head size (CS) 1738 μm [926, 3106]. Color: minor workers concolorous; major workers bicolored: head color dark reddish, tone lighter than that of mesosoma and gaster.

Head: Ground surface smooth, or shagreened, shiny. Head of minor workers often without rugae and rugulae. In major workers postocular surface smooth, or shagreened, shiny, rugae and rugulaeabsent, the preocular head dorsum, genae, and frontal carinae inconspicuously rugulose. Surface around the antennal sockets with concentric rugulae. Anterior clypeal border conspicuously dentate. Clypeus longitudinally costulate, posterior third of clypeus often without costulae. Ground surface smooth or shagreened. Median clypeal costa conspicuous. Frontal triangle inconspicuously sculptured, ground surface smooth, or feebly shagreened, shiny; in major workers lateral parts inconspicuously striate, medially smooth, shiny. In both subcastes median clypeal costa does not surpass the clypeal-frontal triangular border. **Psammophore absent**, only straight or C-shaped hairs present posterior to buccal cavity. Basal scape lobe well-developed (ScBaC/CS 0.045 [0.037, 0.054]), having an acute projection externally.

Mesosoma: feebly sculptured. In minor workers dorsum of pronotum shagreened and shiny, sides shagreened; in major workers dorsum and upper sides of pronotum shagreened, shiny, ventral-most part of the propleuron inconspicuously sculptured, irregularly rugulose, ground surface shagreened, shiny. Mesonotum in minor workers smooth or shagreened, shiny, the ventral-most part of the mesopleuron inconspicuously rugulose transversally; in major workers mesonotum shiny, mesopleuron transversally rugulose, ground surface shagreened, shiny. Propodeum in minor workers smooth or shagreened, shiny, sometimes inconspicuously rugulose; in major workers dorsum and sides transversally, and symmetrically rugose. In both subcastes **propodeum rounded in profile.**

Petiole and Postpetiole: Petiolar node with numerous pairs of long (200–400 μm) hairs. Sides of peduncle with a pair of standing setae longer than 100 μm (100–150 μm).

5.2.1.1. Messor bouvieri. (Fig. 9A–J, Table S1, Table 7)

Relatively small species; Head size (CS) 1400 μm [899, 1832]. Color: minor and major workers concolorous brown to black.

Head: Ground surface smooth, or shagreened. Head of minor workers often without rugae and rugulae; in major workers rugae and rugulaeon head dorsum and postocular sides absent or inconspicuous, ground surface shagreened, dull, sides, genae, and frontal carinae feebly rugulose. Surface around the antennal sockets with concentric rugulae. Anterior clypeal border edentate. Clypeus irregularly sculptured, rugulose, or roguloso-reticulate, ground surface shagreened, dull. Median clypeal costa absent. Frontal triangle longitudinally feebly costulate, ground surface between costulae smooth, or shagreened. **Psammophore, i.e. several pairs of long, J-shaped hairs, posterior to buccal cavity present.** Basal scape lobe weekly developed (ScBaC/CS mean 0.031 [0.025, 0.036]), without acute projection externally.

Mesosoma: Feebly sculptured. Pronotum ground surface shagreened, dull. Sides irregularly rugulose. Mesonotum inconspicuously transversally rugulose, ground surface shagreened, dull. Propodeum transversally, rugulose, ground surface shagreened, dull. Propodeum angulate in profile but does not bear a pair of propodeal tubercles.

Table 7
Mean of morphometric ratios calculated based on individuals for *Messor* species treated in this revisionary work. Morphometric traits are divided by cephalic size (CS, or CL). Means ± standard deviations are provided in the upper row; minimum and maximum values are given in parentheses in the lower row.

	M. barbarus	*M. bouvieri*	*M. capitatus*	*M. erwini* sp. n.
	n = 47	n = 48	n = 45	n = 50
CS	1738 ± 537	1400 ± 215	1787 ± 639	2072 ± 625
	[926, 3106]	[899, 1832]	[936, 3520]	[1150, 3490]
POC/CL	0.339 ± 0.02	0.325 ± 0.02	0.336 ± 0.04	0.360 ± 0.03
	[0.305, 0.385]	[0.310, 0.337]	[0.307, 0.387]	[0.326, 0.395]
FR/CS	0.266 ± 0.01	0.272 ± 0.01	0.270 ± 0.01	0.261 ± 0.01
	[0.248, 0.281]	[0.262, 0.284]	[0.249, 0.294]	[0.226, 0.287]
FL/CS	0.282 ± 0.01	0.295 ± 0.01	0.282 ± 0.01	0.278 ± 0.02
	[0.269, 0.300]	[0.285, 0.307]	[0.253, 0.308]	[0.253, 0.306]
AnScD/CS	0.327 ± 0.01	0.342 ± 0.01	0.337 ± 0.01	0.319 ± 0.02
	[0.300, 0.349]	[0.331, 0.356]	[0.299, 0.364]	[0.290, 0.353]
MW/CS	0.607 ± 0.03	0.628 ± 0.01	0.585 ± 0.03	0.588 ± 0.04
	[0.549, 0.670]	[0.604, 0.659]	[0.503, 0.645]	[0.496, 0.639]
PEW/CS	0.193 ± 0.02	0.213 ± 0.01	0.187 ± 0.02	0.187 ± 0.01
	[0.155, 0.223]	[0.189, 0.244]	[0.161, 0.231]	[0.153, 0.230]
ML/CS	1.256 ± 0.10	1.272 ± 0.04	1.234 ± 0.13	1.217 ± 0.11
	[1.037, 1.404]	[1.195, 1.357]	[0.858, 1.415]	[0.980, 1.361]
MpDep/CS	0.098 ± 0.01	0.094 ± 0.01	0.092 ± 0.01	0.091 ± 0.01
	[0.081, 0.114]	[0.078, 0.122]	[0.068, 0.113]	[0.059, 0.119]
>/CS	0.240 ± 0.02	0.281 ± 0.01	0.257 ± 0.03	0.238 ± 0.02
	[0.194, 0.284]	[0.259, 0.312]	[0.193, 0.306]	[0.199, 0.283]
SL/CS	0.860 ± 0.07	0.860 ± 0.36	0.852 ± 0.09	0.866 ± 0.10
	[0.695, 0.957]	[0.800, 0.950]	[0.650, 0.983]	[0.672, 1.009]
ScBW/CS	0.106 ± 0.01	0.092 ± 0.00	0.100 ± 0.01	0.101 ± 0.01
	[0.085, 0.132]	[0.082, 0.106]	[0.076, 0.119]	[0.077, 0.117]
ScBaC/CS	0.045 ± 0.00	0.031 ± 0.00	0.041 ± 0.01	0.051 ± 0.01
	[0.037, 0.054]	[0.025, 0.036]	[0.032, 0.053]	[0.033, 0.063]
EL/CS	0.194 ± 0.02	0.214 ± 0.01	0.190 ± 0.02	0.170 ± 0.02
	[0.155, 0.242]	[0.197, 0.234]	[0.149, 0.230]	[0.132, 0.210]
PrOc/CS	0.301 ± 0.01	0.300 ± 0.01	0.307 ± 0.01	0.314 ± 0.02
	[0.278, 0.325]	[0.277, 0.325]	[0.290, 0.337]	[0.293, 0.353]

Petiole and Postpetiole: Petiolar node without standing setae. Sides of peduncle with a few pairs of standing setae which are no longer than 100 μm (40–80 μm).

5.2.1.2. Messor capitatus. (Fig. 10A–J, Table S1, Table 7)

Relatively large species; Head size (CS) 1787 μm [936, 3520]. Color: minor and major workers concolorous brown to black.

Head: Ground surface smooth, or shagreened. Head of minor workers often without rugae and rugulae; in major workers rugae and rugulae on head dorsum and postocular sides inconspicuous, ground surface smooth, or shagreened, shiny, sides, genae, and frontal carinae conspicuously rugulose, or rugose. Surface around the antennal sockets with concentric rugulae. Anterior clypeal border conspicuously dentate. Clypeus longitudinally costulate, posterior third of clypeus often without costulae. Ground surface smooth or shagreened. Median clypeal costa conspicuous.

Frontal triangle inconspicuously sculptured. Ground surface smooth, shagreened; in major workers lateral parts irregularly striate, medially smooth. **In both subcastes median clypeal costa does not surpass the clypeal-frontal triangular border**. **Psammophore absent**, only straight or C-shaped hairs present posterior to buccal cavity. Basal scape lobe well-developed (ScBaC/CS 0.041 [0.032, 0.053]), having an acute projection externally.

Mesosoma: feebly sculptured. In minor workers dorsum of pronotum shagreened and moderately shiny, sides shagreened; in major workers dorsum and upper sides of pronotum shagreened, feebly rugulose, ventral-most part of the propleuron inconspicuously sculptured, irregularly rugulose, ground surface shagreened, dull. Mesonotum dorsum and mesopleuron in both subcastes transversally rugose, ground surface punctate or shagreened, dull. Propodeum dorsum and sides in minor workers with very feeble transversal rugulae, ground surface shagreened, moderately shiny sometimes asymmetrically rugose, in major workers dorsum and sides transversally, and symmetrically rugose. Propodeum in minor workers rounded in profile; **in major workers propodeum angulate with a pair of propodeal tubercles**, which are dentiform in the largest workers i.e. sharp longitudinal ridges on the dorsum of propodeal tubercles absent.

Petiole and postpetiole: Petiolar node with numerous pairs of long (200–400 μm) hairs. Sides of peduncle with a pair of standing setae longer than 100 μm (100–150 μm).

5.2.1.3. Messor erwini sp. n.. (Fig. 11A–J, Table S1, Table 7)

Holotype: SPAIN: Castellbell i el Vilar, 41.652909, 1.849238, open and heterogeneous shrubland, June 2018, leg. X. Arnan & R.G. Pol, Collection code #19603. Major worker (Natural History Museum Vienna).

Paratypes: SPAIN: Castellbell i el Vilar, 41.652909, 1.849238, open and heterogeneous shrubland, June 2018, leg. X. Arnan & R.G. Pol, Collection codes #19595, #19597, #19598, #19600, #19601, #19602, #19603, #19604, #19639, #19640, #19641, #19642, #19643, #19645; July 2018, leg. X. Arnan & R.G. Pol, Collection codes #19596, #19599, #19644, #19646. In total, 58 major and minor workers (Hungarian Natural History Museum Budapest, National Museum of Natural History Paris, National Museum of Natural Sciences Madrid, Natural History Museum Basel, Natural History Museum Vienna, private collection of Sándor Csősz).

Etymology: The species is dedicated to Erwin Meyer, wholehearted researcher and teacher of arthropods at the University of Innsbruck for many years, who is greatly missed for his humor, his enthusiasm, and his ability to motivate and to touch hearts.

The largest of the four species analyzed in this study; Head size (CS) 2072 μm [1150, 3490]. Color: minor and smaller major workers concolorous; the largest major workers bicolored: color of head dorsum lighter than head sides, mesosoma and gaster.

Head: Ground surface smooth, or shagreened. In minor workers head often without rugae and rugulae, genae and frons with feeble rugulae, postocular area smooth or shagreened, shiny; in major workers sides, genae, and frontal carinae conspicuously rugulose, or rugose, postocular surface smooth or shagreened, shiny; in the largest major workers postocular part can be inconspicuously rugulose. Surface around the antennal sockets with concentric rugulae. Anterior clypeal border conspicuously dentate. Clypeus longitudinally costulate across the whole area of the clypeus, ground surface smooth or shagreened. Median clypeal costa well-developed and conspicuous. Frontal triangle conspicuously sculptured. Ground surface smooth, or shagreened. **In both subcastes the median clypeal costa always runs across the frontal triangle uninterrupted from the base to the apex**; in minor workers only the median costa is conspicuous; in major workers often a number of well-developed clypeal costae present on the frontal triangle. **Psammophore absent**, only straight or C-shaped hairs present posterior to buccal cavity. Basal scape lobe well-developed (ScBaC/CS 0.051 [0.033, 0.063]), having an acute projection externally.

Mesosoma: coarsely sculptured. In minor workers dorsum of pronotum smooth and shiny, sides smooth, or shagreened, ventral-most part inconspicuously rugulose; in major workers dorsum and propleuron inconspicuously sculptured, longitudinally rugose; in largest major workers rugae and rugulaeconspicuous, ground surface shagreened. Mesonotum dorsum and mesopleuron in both subcastes transversally rugose, ground surface punctate or shagreened, dull. Propodeum dorsum and sides transversally, sometimes asymmetrically rugose. Propodeum in minor workers rounded in profile; **in major workers propodeum angulate with a pair of propodeal tubercles**, which are dentiform or lamelliform in the largest workers, i.e. sharp longitudinal ridges on the dorsum of propodeal tubercles may present.

Petiole and Postpetiole: Petiolar node with numerous pairs of long (200–400 μm) hairs. Sides of peduncle with a pair of standing setae longer than 100 μm (100–150 μm).

Funding

Fieldwork was funded by the Ministério de Ciencia, Innovación y Universidades (grant number RYC-2015-18448).

Declaration of competing interest

The authors declare that they have no known competing financial interests or personal relationships that could have appeared to influence the work reported in this paper.

Data availability

Data will be made available on request.

Acknowledgments

We thank Alba Lázaro-González and Xim Cerdá for providing some colony samples, Xavier Espadaler for checking the first identifications of the *Messor* species, Elisabeth Zangerl for testing the microsatellite primers and her support in the laboratory, Simone Haas and Elisabeth Zangerl for z-stacking photos of worker specimens, Florian Reischer for initializing the GenBank entries, and two anonymous reviewers for constructive criticism of an earlier version of the paper. The computational results presented here have been achieved in part by using the HPC infrastructure of the University of Innsbruck (LEO).

Appendix A. Supplementary data

Supplementary data to this article can be found online at https://doi.org/10.1016/j.jcz.2023.09.001.

References

Abbott, R., Albach, D., Ansell, S., Arntzen, J.W., Baird, S.J.E., Bierne, N., Boughman, J., Brelsford, A., Buerkle, C.A., Buggs, R., Butlin, R.K., Dieckmann, U., Eroukhmanoff, F., Grill, A., Cahan, S.H., Hermansen, J.S., Hewitt, G., Hudson, A.G., Jiggins, C., Jones, J., Keller, B., Marczewski, T., Mallet, J., Martinez-Rodriguez, P., Möst, M., Mullen, S., Nichols, R., Nolte, A.W., Parisod, C., Pfennig, K., Rice, A.M., Ritchie, M.G., Seifert, B., Smadja, C.M., Stelkens, R., Szymura, J.M., Väinölä, R., Wolf, J.B.W., Zinner, D., 2013. Hybridization and speciation. J. Evol. Biol. 26, 229–246. https://doi.org/10.1111/j.1420-9101.2012.02599.x.

Altschul, S.F., Gish, W., Miller, W., Myers, E.W., Lipman, D.J., 1990. Basic local alignment search tool. J. Mol. Biol. 215, 403–410. https://doi.org/10.1016/S0022-2836(05)80360-2.

Arnan, X., Cerdá, X., Retana, J., 2012. Distinctive life traits and distribution along environmental gradients of dominant and subordinate Mediterranean ant species. Oecologia 170, 489–500. https://doi.org/10.1007/s00442-012-2315-y.

Arnan, X., Retana, J., Rodrigo, A., Cerdá, X., 2010. Foraging behaviour of harvesting ants determines seed removal and dispersal. Insectes Sociaux 57, 421–430. https://doi.org/10.1007/s00040-010-0100-7.

Arnan, X., Rodrigo, A., Retana, J., 2006. Post-fire recovery of Mediterranean ground ant communities follows vegetation and dryness gradients. J. Biogeogr. 33, 1246–1258. https://doi.org/10.1111/j.1365-2699.2006.01506.x.

Arthofer, W., Schlick-Steiner, B.C., Steiner, F.M., Konrad, H., Espadaler, X., Stauffer, C., 2005. Microsatellite loci for the study of habitat fragmentation in the harvester ant *Messor structor*. Conserv. Genet. 6, 859–861. https://doi.org/10.1007/s10592-005-9033-5.

Baroni Urbani, C., 1971. Catalogo delle specie di Formicidae d'Italia (Studi sulla mirmecofauna d'Italia X). Memor. Soc. Entomol. Ital. 50, 5–287.

Bernasconi, C., Cherix, D., Seifert, B., Pamilo, P., 2011. Molecular taxonomy of the *Formica rufa* group (red wood ants) (Hymenoptera: Formicidae): a new cryptic species in the Swiss Alps? Myrmecological News 14, 37–47.

Bernhard, F., 1968. Les fourmis (Hymenoptera: Formicidae) d'Europe occidentale et septentrionale. Masson, Paris.

Bickford, D., Lohman, D.J., Sodhi, N.S., Ng, P.K.L., Meier, R., Winker, K., Ingram, K., Das, I., 2007. Cryptic species as a window on diversity and conservation. Trends Ecol. Evol. 22, 148–155. https://doi.org/10.1016/j.tree.2006.11.004.

Bolton, B., 2022. AntCat. An Online Catalog of the Ants of the World. http://antcat.org/. (Accessed 9 August 2022).

Borowiec, L., 2014. Catalogue of ants of Europe, the Mediterranean basin and adjacent regions (Hymenoptera: Formicidae). Genus 25, 1–340.

Cagniant, H., Espadaler, X., 1998. Le genre *Messor* au Maroc (Hymenoptera: Formicidae). Ann. Soc. Entomol. Fr. 33, 419–434.

Cammeraat, L.H., Willott, S.J., Compton, S.G., Incoll, L.D., 2002. The effects of ants' nests on the physical, chemical and hydrological properties of a rangeland soil in semi-arid Spain. Geoderma 105, 1–20. https://doi.org/10.1016/S0016-7061(01)00085-4.

Cerdá, X., Retana, J., 1994. Food exploitation patterns of two sympatric seed-harvesting ants *Messor bouvieri* (Bond.) and *Messor capitatus* (Latr.) (Hym., Formicidae) from Spain. J. Appl. Entomol. 117, 268–277. https://doi.org/10.1111/j.1439-0418.1994.tb00735.x.

Chialvo, P., Gotzek, D.A., Shoemaker, D., Ross, K.G., 2018. Genetic analyses reveal cryptic diversity in the native North American fire ants (Hymenoptera: Formicidae: *Solenopsis*). Syst. Entomol. 43, 109–122. https://doi.org/10.1111/syen.12254.

Collingwood, C.A., 1976. A provisional list of Iberian Formicidae with a key to the worker caste. Eos 52, 65–95.

Collingwood, C.A., 1998. A Guide to Ants of Continental Portugal (Hymenoptera: Formicidae). Sociedade Portuguesa de Entomologia, Lisboa.

Cordonnier, M., Gayet, T., Escarguel, G., Kaufmann, B., 2019. From hybridization to introgression between two closely related sympatric ant species. J. Zool. Syst. Evol. Res. 57, 778–788. https://doi.org/10.1111/jzs.12297.

Csősz, S., Fisher, B.L., 2016. Taxonomic revision of the Malagasy members of the Nesomyrmex angulatus species group using the automated morphological species delineation protocol NC-PART-clustering.. PeerJ 4, e1796. https://doi.org/10.7717/peerj.1796.

Csősz, S., Seifert, B., Müller, B., Trindl, A., Schulz, A., Heinze, J., 2014. Cryptic diversity in the Mediterranean *Temnothorax lichtensteini* species complex (Hymenoptera: Formicidae). Org. Divers. Evol. 14, 75–88. https://doi.org/10.1007/s13127-013-0153-3.

Dejaco, T., Gassner, M., Arthofer, W., Schlick-Steiner, B.C., Steiner, F.M., 2016. Taxonomist's nightmare ... evolutionist's delight: an integrative approach resolves species limits in jumping bristletails despite widespread hybridization and parthenogenesis. Syst. Biol. 65, 947–974. https://doi.org/10.1093/sysbio/syw003.

Donoghue, M.J., 1985. A critique of the biological species concept and recommendations for a phylogenetic alternative. Bryol. 88, 172–181.

Earl, D.A., von Holdt, B.M., 2012. Structure HARVESTER: a website and program for visualizing STRUCTURE output and implementing the Evanno method. Conserv. Genet. Res. 4, 359–361. doi: 10.1007/s12686-011-9548-7.

Evanno, G., Regnaut, S., Goudet, J., 2005. Detecting the number of clusters of individuals using the software STRUCTURE: a simulation study. Mol. Ecol. 14, 2611–2620. https://doi.org/10.1111/j.1365-294X.2005.02553.x.

Eyer, P.A., Hefetz, A., 2018. Cytonuclear incongruences hamper species delimitation in the socially polymorphic desert ants of the *Cataglyphis albicans* group in Israel. J. Evol. Biol. 31, 1828–1842. https://doi.org/10.1111/jeb.13378.

Eyer, P.A., Seltzer, R., Reiner-Brodetzki, T., Hefetz, A., 2017. An integrative approach to untangling species delimitation in the *Cataglyphis bicolor* desert ant complex in Israel. Mol. Phylogenet. Evol. 115, 128–139. https://doi.org/10.1016/j.ympev.2017.07.024.

Felsenstein, J., 1985. Confidence limits on phylogenies: an approach using the bootstrap. Evolution 39, 783–791. https://doi.org/10.1111/j.1558-5646.1985.tb00420.x.

Fiedler, K., Kuhlmann, F., Schlick-Steiner, B.C., Steiner, F.M., Gebauer, G., 2007. Stable N-isotope signatures of central European ants – assessing positions in a trophic gradient. Insect. Soc. 54, 393–402. https://doi.org/10.1007/s00040-007-0959-0.

Folmer, O., Black, M., Hoeh, W., Lutz, R., Vrijenhook, R., 1994. DNA primers for amplification of mitochondrial cytochrome c oxidase subunit I from diverse metazoan invertebrates. Mol. Mar. Biol. Biotechnol. 3, 294–299.

Gómez, K., Espadaler, X., 2007. Hormigas Ibéricas. http://www.hormigas.org. (Accessed 15 April 2020).

Gompert, Z., Fordyce, J.A., Forister, M.L., Shapiro, A.M., Nice, C.C., 2006. Homoploid hybrid speciation in an extreme habitat. Science 314, 1923–1925. https://doi.org/10.1126/science.1135875.

Hölldobler, B., Wilson, E.O., 1990. The Ants. Springer, Berlin.

Kalinowski, S.T., 2011. The computer program STRUCTURE does not reliably identify the main genetic clusters within species: simulations and implications for human population structure. Heredity 106, 625–632. https://doi.org/10.1038/hdy.2010.95.

Knaden, M., Tinaut, A., Cerda, X., Wehner, S., Wehner, R., 2005. Phylogeny of three parapatric species of desert ants, *Cataglyphis bicolor, C. viatica* and *C. savignyi*: a comparison of mitochondrial DNA, nuclear DNA, and morphological data. Zoology 108, 169–177. https://doi.org/10.1016/j.zool.2005.03.005.

Koffi, K.G., Heuertz, M., Doumenge, C., Onana, J.M., Gavory, F., Hardy, O.J., 2010. A combined analysis of morphological traits, chloroplast and nuclear DNA sequences within *Santiria trimera* (Burseraceae) suggests several species following the Biological Species Concept. Plant Ecology and Evolution 143, 160–169. https://doi.org/10.1146/annurev.ecolsys.30.1.327.

Kofler, R., Schlötterer, C., Lelley, T., 2007. SciRoKo: a new tool for whole genome microsatellite search and investigation. Bioinformatics 23, 1683–1685. https://doi.org/10.1093/bioinformatics/btm157.

Kumar, S., Stecher, G., Tamura, K., 2016. MEGA7: molecular evolutionary genetics analysis version 7.0 for bigger datasets. Mol. Biol. Evol. 33, 1870–1874. https://doi.org/10.1093/molbev/msw054.

Lebas, C., Galkowski, C., Blatrix, R., Wegnez, P., 2016. Fourmis d'Europe Occidentale. Le Premier Guide Complet d'Europe. Delachaux et Niestle, Paris.

Lucas, C., Fresneau, D., Kolmer, K., Heinze, J., Delabie, J.H.C., Pho, D.B., 2002. A multidisciplinary approach to discriminating different taxa in the species complex *Pachycondyla villosa* (Formicidae). Biol. J. Linn. Soc. 75, 249–259. https://doi.org/10.1046/j.1095-8312.2002.00017.x.

Maechler, M., Rousseeuw, P., Struyf, A., Hornik, K., 2014. Cluster: Cluster Analysis Basics and Extensions. R package version 1.15.3.(Accessed November 2018).

Mallet, J., 1995. A species definition for the modern synthesis. Trends Ecol. Evol. 10, 294–299. https://doi.org/10.1016/0169-5347(95)90031-4.

Mallet, J., 2005. Hybridization as an invasion of the genome. Trends Ecol. Evol. 20, 229–237. https://doi.org/10.1016/j.tree.2005.02.010.

McCarthy, C., 1996. Chromas. School of Biomolecular and Biomedical Science. Griffith University, Brisbane, Queensland. https://technelysium.com.au/wp/chromas/. (Accessed November 2018).

Nei, M., Kumar, S., 2000. Molecular Evolution and Phylogenetics. Oxford University Press, New York.

Nilsen, G., Lingjaerde, O.C., 2013. clusterGenomics: identifying clusters in genomics data by recursive partitioning. R package version 1.0. http://CRAN.R-project.org/package=clusterGenomics. (Accessed 10 January 2017).

Norman, V., Darras, H., Tranter, C., Aron, S., Hughes, W.O.H., 2016. Cryptic lineages hybridize for worker production in the harvester ant *Messor barbarus*. Biol. Lett. 12, 1–5. https://doi.org/10.1098/rsbl.2016.0542.

Plowes, N.J.R., Johnson, R.A., Hölldobler, B., 2013. Foraging behavior in the ant genus *Messor* (Hymenoptera: Formicidae: Myrmicinae). Myrmecological News 18, 33–49.

Pritchard, J.K., Stephens, M., Donnelly, P., 2000. Inference of population structure using multilocus genotype data. Genetics 155, 945–959.

Puechmaille, S.J., 2016. The program STRUCTURE does not reliably recover the correct population structure when sampling is uneven: subsampling and new estimators alleviate the problem. Mol. Ecol. Res. 16, 608–627. https://doi.org/10.1111/1755-0998.12512.

Queiroz, K. de, 2007. Species concepts and species delimitation. Syst. Biol. 56, 879–886. https://doi.org/10.1080/10635150701701083.

R Development Core Team, 2020. R: a Language and Environment for Statistical Computing. R Foundation for Statistical Computing, Vienna, Austria.

Raymond, M., Rousset, F., 1995. GENEPOP (version 1.2): population genetics software for exact tests and ecumenicism. J. Hered. 86, 248–249.

Romiguier, J., Fournier, A., Yek, S.H., Keller, L., 2017. Convergent evolution of social hybridogenesis in *Messor* harvester ants. Mol. Ecol. 26, 1108–1117. https://doi.org/10.1111/mec.13899.

Ronque, M.U.V., Azevedo-Silva, M., Mori, G.M., Souza, A.P., Oliveira, P.S., 2016. Three ways to distinguish species: using behavioural, ecological, and molecular data to tell apart two closely related ants, *Camponotus renggeri* and *Camponotus rufipes* (Hymenoptera: Formicidae). Zool. J. Linn. Soc. 176, 170–181. https://doi.org/10.1111/zoj.12303.

Ronquist, F., Teslenko, M., van der Mark, P., Ayres, D.L., Darling, A., Hohna, S., Larget, B., Liu, L., Suchard, M.A., Huelsenbeck, J.P., 2012. MrBayes 3.2: efficient Bayesian phylogenetic inference and model choice across a large model space. Syst. Biol. 61, 539–542. https://doi.org/10.1093/sysbio/sys029.

Ross, K.G., Gotzek, D., Ascunce, M.S., Shoemaker, D.D., 2010. Species delimitation: a case study in a problematic ant taxon. Syst. Biol. 59, 162–184. https://doi.org/10.1093/sysbio/syp089.

Rousset, F., 2008. Genepop'007: a complete reimplementation of the genepop software for windows and linux. Mol. Ecol. Res. 8, 103–106. https://doi.org/10.1111/j.1471-8286.2007.01931.x.

Saitou, N., Nei, M., 1987. The neighbor-joining method: a new method for reconstructing phylogenetic trees. Mol. Biol. Evol. 4, 406–425. https://doi.org/10.1093/oxfordjournals.molbev.a040454.

Schlick-Steiner, B.C., Steiner, F.M., Konrad, H., Markó, B., Csősz, S., Heller, G., Ferencz, B., Sipos, B., Christian, E., Stauffer, C., 2006. More than one species of *Messor* harvester ants (Hymenoptera: Formicidae) in central Europe. Eur. J. Entomol. 103, 469–476. https://doi.org/10.14411/eje.2006.060.

Schlick-Steiner, B.C., Steiner, F.M., Seifert, B., Stauffer, C., Christian, E., Crozier, R.H., 2010. Integrative taxonomy: a multisource approach to exploring biodiversity. Annu. Rev. Entomol. 55, 421–438. https://doi.org/10.1146/annurev-ento-112408-085432.

Seifert, B., 1999. Interspecific hybridisations in natural populations of ants by example of a regional fauna (Hymenoptera, Formicidae). Insect. Soc. 46, 45–52. https://doi.org/10.1007/s000400050111.

Seifert, B., 2018. The Ants of Central and North Europe. lutra Verlags- und Vertriebsgesellschaft, Tauer, Germany. ISBN 9783936412079.

Seifert, B., 2019a. Hybridization in the European carpenter ants *Camponotus herculeanus* and *C. ligniperda* (Hymenoptera: Formicidae). Insectes Sociaux 66, 365–374. https://doi.org/10.1007/s00040-019-00693-0.

Seifert, B., 2019b. *Lasius nigroemarginatus* Forel, 1874 is a F1 hybrid between *L. emarginatus* (Olivier, 1792) and *L. platythorax* Seifert, 1991 (Hymenoptera, Formicidae). Beiträge zur Entomologie = Contributions to Entomology 69, 291–300. https://doi.org/10.21248/contrib.entomol.69.2.291-300.

Seifert, B., Csösz, S., Schulz, A., 2014. NC-Clustering demonstrates heterospecificity of the cryptic ant species Temnothorax luteus (FOREL, 1874) and T. racovitzai (BONDROIT, 1918) (Hymenoptera: Formicidae). Contrib. Entomol. 64, 47–57. https://doi.org/10.21248/contrib.entomol.64.1.47-57.

Simon, C., Frati, F., Beckenbach, A., Crespi, B., Liu, H., Flook, P., 1994. Evolution, weighting, and phylogenetic utility of mitochondrial gene sequences and a compilation of conserved polymerase chain reaction primers. Ann. Entomol. Soc. Am. 87, 651–701. https://doi.org/10.1093/aesa/87.6.651.

Solida, L., Scalisi, M., Fanfani, A., Mori, A., Grasso, D.A., 2010. Interspecific space partitioning during the foraging activity of two syntopic species of *Messor* harvester ants. J. Biol. Res. 13, 3–12.

Steiner, F.M., Csősz, S., Markó, B., Gamisch, A., Rinnhofer, L., Folterbauer, C., Hammerle, S., Stauffer, C., Arthofer, W., Schlick-Steiner, B.C., 2018. Turning one into five: integrative taxonomy uncovers complex evolution of cryptic species in the harvester ant *Messor "structor"*. Mol. Phylogenet. Evol. 127, 387–404. https://doi.org/10.1016/j.ympev.2018.04.005.

Steiner, F.M., Seifert, B., Grasso, D.A., Le Moli, F., Arthofer, W., Stauffer, C., Crozier, R.H., Schlick-Steiner, B.C., 2011. Mixed colonies and hybridisation of *Messor* harvester ant species (Hymenoptera: Formicidae). Org. Divers. Evol. 11, 107–134. https://doi.org/10.1007/s13127-011-0045-3.

Struck, T.H., Feder, J.L., Bendiksby, M., Birkeland, S., Cerca, J., Gusarov, V.I., Kistenich, S., Larsson, K.-H., Liow, L.H., Nowak, M.D., Stedje, B., Bachmann, L., Dimitrov, D., 2018. Finding evolutionary processes hidden in cryptic species. Trends Ecol. Evol. 33, 153–163. https://doi.org/10.1016/j.tree.2017.11.007.

Thompson, J.D., Gibson, T.J., Plewniak, F., Jeanmougin, F., Higgins, D.G., 1997. The CLUSTAL_X windows interface: flexible strategies for multiple sequence alignment aided by quality analysis tools. Nucleic Acids Res. 25, 4876–4882. https://doi.org/10.1093/nar/25.24.4876.

Tibshirani, R., Walther, G., Hastie, T., 2001. Estimating the number of clusters in a data set via the gap statistic. J. Roy. Stat. Soc. B 63, 411–423. https://doi.org/10.1111/1467-9868.00293.

Venables, W.N., Ripley, B.D., 2002. Modern Applied Statistics with S, fourth ed. Springer, New York. ISBN 0-387-95457-0.

Wagner, H.C., Gamisch, A., Arthofer, W., Moder, K., Steiner, F.M., Schlick-Steiner, B.C., 2018. Evolution of morphological crypsis in the *Tetramorium caespitum* ant species complex (Hymenoptera: Formicidae). Sci. Rep. 8, 12547 https://doi.org/10.1038/s41598-018-30890-z.

Westerman, P.R., Atanackovic, V., Royo-Esnal, A., Torra, J., 2012. Differential weed seed removal in dryland cereals. Arthropod-Plant Interactions 6, 591–599. https://doi.org/10.1007/s11829-012-9211-6.

Wiens, J.J., 1999. Polymorphism in systematics and comparative biology. Annu. Rev. Ecol. Evol. Syst. 30, 327–362. https://doi.org/10.1146/annurev.ecolsys.30.1.327.